Measurement reports

Spatial variability of northern Iberian rainfall stable isotope values: Investigating atmospheric controls on daily and monthly timescales

Ana Moreno[1], Miguel Iglesias[2], Cesar Azorin-Molina[3], Carlos Pérez-Mejías[4,1], Miguel Bartolomé[5,6], Carlos Sancho[Ŧ], Heather Stoll[7], Isabel Cacho[8], Jaime Frigola[8], Cinta Osácar[5], Arsenio Muñoz[5], Antonio Delgado-Huertas[9], Ileana Bladé[10] and Françoise Vimeux[11,12]

[1]Department of Geoenvironmental Processes and Global Change, Pyrenean Institute of Ecology – CSIC, Avda. Montañana 1005, 50059 Zaragoza, Spain

[2]Department of Geology, University of Oviedo, C/Arias de Velasco, s/nº 33005 Oviedo, Spain

[3]Centro de Investigaciones sobre Desertificación, Consejo Superior de Investigaciones Científicas (CIDE-CSIC), Moncada 46113, Valencia, Spain

[4]Institute of Global Environmental Change, Xi'an Jiaotong University, Xi'an, 710049, China

[5]Earth Sciences Department, University of Zaragoza, C/Pedro Cerbuna 12, 50009 Zaragoza, Spain

[6]Departamento de Geología. Museo Nacional de Ciencias Naturales – CSIC, C/José Gutiérrez Abascal 2, 28006, Madrid, Spain

[7]Geological Institute, NO G59, Department of Earth Sciences, Sonneggstrasse 5, ETH, 8092 Zurich, Switzerland

[8]CRG Marine Geosciences, Department de Dinàmica de la Terra i l'Oceà, Facultat de Ciències de la Terra, Universitat de Barcelona, C/Martí i Franqués, s/nº, 08028 Barcelona, Spain

[9]Stable Isotope Biogeochemistry Laboratory, IACT-CSIC, Avda. de Las Palmeras nº 4, 18100, Armilla (Granada) Spain

[10]Group of Meteorology, Department of Applied Physics, Faculty of Physics, University of Barcelona, Martí i Franqués,1, 08028 Barcelona, Spain

[11] HydroSciences Montpellier (HSM), UMR 5569 (UM, CNRS, IRD), 34095 Montpellier, France.

[12]Institut Pierre Simon Laplace (IPSL), Laboratoire des Sciences de Climat et de l'Environnement (LSCE), UMR 8212 (CEA, CNRS, UVSQ), 91191 Gif-sur-Yvette, France.

[Ŧ] Deceased, February 2019

Correspondence to: Cesar Azorin-Molina (cesar.azorin@uv.es)

Abstract. This article presents for the first time a large dataset of rainfall isotopic measurements ($\delta^{18}O_p$ and $\delta^{2}H_p$), sampled every day or two days from seven sites on a west-to-east transect across northern Spain for 2010-2017. The main aim of this study is to: (1) characterize the rainfall isotopic variability in northern Spain at daily and monthly time scales, and (2) assess the principal factors influencing rainfall isotopic variability. The relative role of air temperature and rainfall in determining the stable isotope composition of precipitation changes along the west-to-east transect, being air temperature highly correlated with $\delta^{18}O_p$ at daily and monthly time scales while a few sites along the transect show a significant negative correlation with precipitation. The highest air temperature-$\delta^{18}O_p$ dependency is found for a station located in the Pyrenees. Frontal systems associated with North Atlantic cyclones are the dominant mechanism inducing precipitation in this region, particularly in winter. This study allows an exploration of the role of air mass source and trajectory in determining the isotopic composition of rainfall in northern Iberia by characterizing the moisture uptake for three of the seven stations. The importance of continental versus marine moisture sources is evident, with clear seasonal and spatial variations. In addition, the type of precipitation (convective versus frontal rainfall) plays a key role, with convective rainfall associated with higher $\delta^{18}O_p$ values. This comprehensive spatio-temporal approach to analyzing the rainfall isotopic composition represents another step forward towards developing a more detailed, mechanistic framework for interpreting stable isotopes in rainfall as a palaeoclimate and hydrological tracer.

1 Introduction

The oxygen isotopic composition of rainfall ($\delta^{18}O_p$) is often considered the dominant influence on the isotopic composition of terrestrial archives (ice cores, speleothems or authigenic lacustrine carbonates) used to reconstruct past climate (e.g., Leng, 2006). However, few palaeoclimate reconstructions are supported by an in-depth understanding of the regional climatic controls on $\delta^{18}O_p$ (e.g. Treble et al., 2005). As a consequence, palaeoclimate proxies are often interpreted without a clear knowledge of the processes involved in modulating $\delta^{18}O_p$ in a particular region (López-Blanco et al., 2016; Moreno et al., 2017). It has long been established that $\delta^{18}O_p$ is an integrated product of air mass history, modulated by specific prevailing meteorological conditions, in particular, air temperature and amount of precipitation (Craig, 1961; Dansgaard, 1964). This implies that several dominant factors may control $\delta^{18}O_p$ variability depending on the site location, i.e., latitude, continentality, elevation, seasonal distribution, local air temperature, and the amount and source of precipitation (Rozanski et al., 1993). A detailed study of current $\delta^{18}O_p$ values and their variability in a given region is essential to reconstructing past climate changes using $\delta^{18}O$ in regional climate archives (Lachniet, 2009).

Long rainfall isotopic time series allow for comparison of the $\delta^{18}O_p$ signal with meteorological variables and calibration of proxy records. Unfortunately such long-term observational studies are scarce, and thus, only a few, albeit outstanding, examples of studies examining factors controlling $\delta^{18}O_p$ are available for continental Europe (Field, 2010; Genty et al., 2014; Tyler et al., 2016). Yet, results obtained for European regions mostly under the influence of rainfall with Atlantic origin (e.g., Baldini et al., 2010) cannot be directly applied to the Iberian Peninsula (IP), where three major weather precipitation regimes coexist (Millán et al., 2005) and where a potential for palaeoclimate reconstructions exists via speleothems derived proxies. Previous studies have shown that the spatial distribution of $\delta^{18}O_p$ and $\delta^{2}H_p$ on monthly time scales in Spain can be approached by a simple multiple regression model, based only on two geographic factors: latitude and elevation (Díaz et al., 2007; Díaz-Tejeiro et al., 2013). However, this model does not reproduce the observed distribution of stable isotope precipitation composition with detailed spatial resolution. The well-known complex topography and varied weather regimes of the Iberian Peninsula (AEMET and Instituto de Meteorologia de Portugal, 2011; Martin-Vide and Olcina-Cantos, 2001) require more targeted studies that take into account the high spatial variability of $\delta^{18}O_p$ in Iberia and the multiple (and sometimes overlapping) processes determining its temporal variation.

A major advance in understanding the controls on $\delta^{18}O_p$ has been the proliferation of studies using daily-scale monitoring to address the mechanisms behind isotopic signatures at daily timescales (Baldini et al., 2010; Fischer and Baldini, 2011), which incorporate the complexity associated with the different types of rainfall (eg. frontal or convective system) (Aggarwal et al., 2016). Regrettably, the scarcity of *Global Network of Isotopes in Precipitation* (hereafter GNIP) sites in Iberia, particularly those using data at daily time scales, prevents a broader regional study of climate controls on $\delta^{18}O_p$ values. In the IP, only one study has analysed $\delta^{18}O_p$ variability on a daily basis over a short 3-year period (2000-2002) (Araguás-Araguás and Diaz Teijeiro, 2005) and, more recently, a 3-year monitoring survey focused on the Iberian Range (Molinos Cave, Teruel, NE Spain) (Moreno et al., 2014). That study revealed the importance of the *source effect* on $\delta^{18}O_p$ values, due to the alternating influence of two air masses with different origins and different isotopic ranges. Atlantic fronts, which are associated with more negative $\delta^{18}O_p$ values (from the west), and Mediterranean convective storms, with more positive values (eastern sources) (Moreno et al., 2014). Additionally, another recent study based on back trajectories emphasized the role of recycled moisture uptake within the IP in the final values of $\delta^{18}O_p$ in Central Spain (Eagle Cave) (Krklec and Domínguez-Villar, 2014). Besides those studies based on $\delta^{18}O_p$, another recent work focused on trace elements in precipitation at two Pyrenean sites reveals the importance of seasonality in the role played by continental vs. marine sources of moisture (Suess et al., 2019). In addition, to date, the majority of empirical studies of meteorological controls over $\delta^{18}O_p$ are based on event,daily, or monthly time series from individual locations (Moreno et al., 2014; Smith et al., 2016). The scarce studies dealing with multiple sampling locations span areas under the influence of the same climatic regime (Baldini et al., 2010; Jeelani et al., 2018). This approach raises concerns about the spatial representativeness of the resulting statistical models and the mechanisms behind the identified relationships in areas as complex as the IP.

In this paper we present a comprehensive analysis of daily and monthly patterns of $\delta^{18}O_P$ from *multiple* stations across northern IP all the way to the Balearic Islands, following an 850-km long west-to-east transect that extends from an area dominated by a typical Atlantic climate to one dominated by a Mediterranean climate. The overall aim is to characterize the dominant factors modulating $\delta^{18}O_p$ variations in time (daily and monthly) and space, in order to determine the causes of regional precipitation isotope variations. The role of geographic factors (continental and elevation effects) and atmospheric processes (moisture origin and type of rainfall) is evaluated. Additionally, this study will serve to improve the interpretation of oxygen isotope paleo-records from northern IP that depend on $\delta^{18}O_p$ (Bartolomé et al., 2015; Domínguez-Villar et al., 2017; López-Blanco et al., 2016; Pérez-Mejías et al., 2019; Sancho et al., 2018, 2015).

2 Weather regime, climate and site description

Our study compares, for the first time, rainfall isotopic values and meteorological variables (air temperature, precipitation, moisture source and type of rainfall) at seven sites in northern Iberia and Balearic Islands, covering an 850-km long west-to-east transect from an area under typical Atlantic climate (Oviedo and El Pindal) to a fully Mediterranean climate (Mallorca Island and Barcelona). The west-to-east transect is completed with three additional sites in a transitional zone: two from the Iberian Range (Molinos and Ortigosa de Cameros) and one from the Pyrenees (Borrastre) (Figure 1a). At those seven locations, rainfall was sampled on daily basis except at El Pindal where it was collected every 48h (Table 1). The Borrastre record is, to our knowledge, the most comprehensive dataset of daily $\delta^{18}O_p$ for Spain in terms of both time span covered (2011-2016) and number of samples (380 days) (Table S1).

In north-western and north-central Iberia, precipitation is mainly controlled by the presence of westerly winds and the passage of Atlantic fronts, especially during November-April (Martín-Vide and Olcina Cantos, J., 2001; Rüdisühli et al., 2020). During the rest of the year, the subtropical Azores high-pressure system shifts northward, which blocks the westerly circulation and moisture inflow from Atlantic sources (Archer and Caldeira, 2008), thus favouring stable atmospheric conditions and reducing precipitation. This wet winter/dry summer regime is quite different from that in the north-eastern Mediterranean region of Iberia, where winters are generally dry whereas in the warm season (from late spring to early autumn) precipitation is more abundant and dominated by convective storms and also fronts that approach the IP from the east (backdoor cold fronts) (Millán et al., 2005). These mesoscale circulation is primarily associated with frequent and persistent sea breezes (Azorin-Molina et al., 2011), which bring warm and moist air masses from the Mediterranean sea inland (Azorin-Molina et al., 2009). During the summer season, this is typically the only source of precipitation in the north-eastern IP, bringing an average of 100-125 mm yearly (Millán et al., 2005). Backdoor cold fronts from the Mediterranean Sea are sporadic events occurring mainly in autumn (and to a lesser extent in winter-spring), but that can cause heavy precipitation and flooding (Llasat et al., 2007). Figure 1B summarizes these three major precipitation regimes defined by Millán et al. (2005): (i) Atlantic frontal systems (westerly winds), (ii) convective–orographic storms, and (iii) Backdoor cold fronts from the Mediterranean Sea (easterly winds).

Below, the seven studied stations are grouped into four regions and described in terms of their climatology.

The Cantabrian coast. The sites of El Pindal and Oviedo in the Cantabrian coast (Figure 1A) are characterized by a typical oceanic climate with mild summers and winters (Cfb, following Köppen and Geiger – KGC- classification) due to the proximity to the coast. Rainfall occurs along the whole year with a minimum in summer and is associated with Atlantic frontal systems (westerly winds).

The Iberian Range. Ortigosa de Cameros is located in the Encinedo Mountain area in the westernmost sector of the Cameros Range (Iberian Range, Figure 1A) and is dominated by a continental Mediterranean climate (Dsb, following KGC classification). Rainfall occurs mostly in autumn and spring, with some convective-orographic storms in summer. The Molinos site is also located in the Iberian Range and at similar elevation but further east, in the Maestrazgo basin. It is characterized by a similar climate (Dsb in KGC classification), with a highly pronounced seasonality; precipitation occurs mainly in spring and autumn.

The Pyrenees. Borrastre village is located in the Central Pyrenees (Figure 1A) and has a transitional climate Mediterranean-Oceanic (Csb in KGC classification), with precipitation occurring mainly in spring and, to a lesser extent, in autumn, exhibiting a mix of the three Atlantic, Mediterranean and convective precipitation regimes.

The Mediterranean. The typical Mediterranean climate (Csa in KGC classification) is represented by the Manacor and Porto Cristo localities in the Mallorca island and by Barcelona (Figure 1A). Precipitation is mostly distributed from October to April typically associated with backdoor cold fronts from the Mediterranean Sea (easterly winds) as the influence of Atlantic precipitation is weak over this area.

3 Analytical and statistical methods

3.1 Sampling

Rainwater was collected using a similar procedure to that recommended by the International Atomic Energy Agency (IAEA) for daily sampling (http://www-naweb.iaea.org/napc/ih/IHS_resources_gnip.html) for six of the seven stations (Oviedo, Ortigosa de Cameros, Molinos, Borrastre, Mallorca and Barcelona). Precipitation events greater than or equal to 1 mm were sampled manually from the water accumulated in the rain gauge using a syringe. The collected water was then homogenized and filtered at the time of sampling; later a 5 ml aliquot was stored in polypropylene tubes sealed with screwcup without air inside and kept cold in a refrigerator until be analyzed. Rainfall samples were collected at the end of each precipitation event, immediately afterwards whenever possible or after a few hours, with the total event precipitation homogenized. At El Pindal site the procedure was different: rainfall was collected every 48h for several months (November 2006 to April 2009, a total of 101 samples) using an automated self-built revolver-type sampler that contained twenty-four 1L Nalgene bottles, thus avoiding any mixing of subsequent samples (see Fischer et al., 2019). A film of paraffin oil was used to prevent evaporation. It was located on the roof of the San Emeterio lighthouse located <10 m from the modern sea cliff (Table 1).

The observation staff in charge of each location collected a sample directly following every rainfall event, except in El Pindal that has an automatic system and in Mallorca, where several events were missed during the first two years of the collection period, preventing the calculation of monthly averages for some intervals (monthly and annual averages and standard deviations in Table 2). Thus, 47 rainfall samples were collected from Oviedo manually in 2015. In Ortigosa de Cameros, rainfall was manually collected daily between September 2010 and December 2014 by the staff (guides) of the La Viña and La Paz show caves, with an interruption from December 2012 – January 2014 (total of 193 samples). In Molinos, rainfall was manually collected by the staff of the Grutas de Cristal cave every day for just over five years (March 2010-May 2015, 268 samples). The first 3 years rainfall data from that survey was previously published (Moreno et al., 2014; Pérez-Mejías et al., 2018). In Borrastre, rainfall was manually collected daily using a Hellman rain gauge from April 2011 to May

2016 (380 events). In Barcelona, rainfall samples were manually obtained from the weather station on the roof of the School of Physics of the University of Barcelona using a standard rain gauge (53 samples). In addition, 98 rainfall events were collected in Mallorca, 7 were replicated at two different localities (Manacor and Porto Cristo) obtaining similar $\delta^{18}O_p$ results. For those 7 events, a weighted-average value using the two localities was calculated (see Table S1).

3.2 Analytical methods

The isotopic composition of oxygen and hydrogen in rainfall samples are expressed as $\delta^{18}O$ and δ^2H in ‰ relative to Vienna Standard Mean Ocean Water (VSMOW). Molinos, Borrastre and most of Ortigosa de Cameros samples (143 samples) were analysed using a Finningan Delta Plus XL mass spectrometer at the IACT-CSIC in Granada. Water samples were equilibrated with CO_2 for the analysis of $\delta^{18}O$ values (Epstein and Mayeda, 1953), while the hydrogen isotopic ratios were measured on H_2 produced by the reaction of 10 µL of water with metallic zinc at 500°C, following the analytical method of Coleman et al. (1982). The analytical error for $\delta^{18}O$ and δ^2H was ±0.1 and ±1 ‰, respectively. The Mallorca and Barcelona samples and the remaining samples from Ortigosa de Cameros (50 samples) were analysed at the Scientific and Technological Centre from the University of Barcelona, δ^2H via TCEA pyrolysis coupled to Thermo Delta Plus XP mass spectrometer and $\delta^{18}O$ with a MAT 253 Thermofisher spectrometer coupled with a gas bench. The analytical error for $\delta^{18}O$ and δ^2H was ±0.2 and ±1.5 ‰ respectively. El Pindal samples were measured at three different laboratories (see Stoll et al., 2015, for more details). Rainfall collected from November 2006 through the end of February 2007 was analysed at the University of Barcelona using the procedure described above. Rainfall collected from June 2007 to May 2008 was analysed in the Marine Biological Laboratories of the University of Oviedo, using equilibration with CO_2 on GV Multiflow-Bio unit coupled to a GV ISOPRIME CF mass spectrometer. Rainfall collected from June 2008 to April 2009 and samples from 2015 were analysed using equilibration with CO_2 on Gas Prep unit coupled to a Nu Instruments Horizon mass spectrometer at the University of Oviedo. Uncertainties are ±0.1‰ (1s) for $\delta^{18}O$ and ±1 %.for δ^2H, based on replicate analyses. Unfortunately, no comparison was made between the different involved laboratories and thus the study does not account for possible offsets between them.

Additionally, 18 samples of potentially evaporated water with abnormally high values in $\delta^{18}O_p$ - and that occurred in summer months when maximum daily air temperatures exceeded 30°C - were classified as outliers and removed from the database. These 18 samples (Table S1) were from Ortigosa de Cameros (4 samples), Borrastre (6 samples) and Molinos (8 samples). Partial evaporation of falling rain-droplets is an alternative interpretation for the high $\delta^{18}Op$ values of these samples.

3.3 Meteorological data

Air temperature and precipitation (on daily and monthly time scales) were obtained from the closest meteorological stations over the sampling periods, as indicated in Table 1, to investigate the statistical relationship with isotopic values. For Oviedo, meteorological data are obtained from Oviedo AEMET station. For El Pindal (120 km from Oviedo; 70 km from Santander), since there were no good data from nearby stations, we decided to use ERA-Interim re-analysis from the European Center for Medium-range Weather Forecasts (ECMWF), which provides gridded weather data (Berrisford et al., 2009; Dee et al., 2011). For Ortigosa site, meteorological data were obtained from the Villoslada de Cameros meteorological station (http://www.larioja.org/ emergencias-112/es/meteorologia), 6.5 km far from the rainfall collection site. The Borrastre sampling site has its own meteorological station (http://borrastre.dyndns.org/MeteoBorrastre) (Table 1), but for the first 22 events data were obtained from ERA-Interim since the station was not yet operative. Finally, for Mallorca we used data from the Sant Llorenç station (8 km), while Barcelona meteorological data are obtained from Zona Universitaria station (www.meteo4u.com).

3.4 Statistical analyses

Prior to conducting correlation analysis at daily time scales, we removed the seasonal cycle of the variables by subtracting their monthly averages to avoid sympathetic seasonal correlations (e.g. Kawale et al., 2011; Rozanski et al., 1993) (Table 3A). To establish correlations on the monthly scale with meteorological variables (Table 3B), $\delta^{18}O_p$ monthly averages weighted by the amount of precipitation were calculated using the following formula:

$$\delta^{18}O_{monthly} = ((Q1 \text{ x } \delta^{18}O_1) + (Q2 \text{ x } \delta^{18}O_2) \ldots (Q_i \text{ x } \delta^{18}O_i)) / (Q_1+Q_2 + \ldots Q_i) \quad [1]$$

where Q = rainfall quantity for day i (in mm). Daily values were not averaged since there was only one rainfall sample per day resulting from the homogenization of all event samples from that day. Spearman's rank correlation analysis, a non-parametric measure alternative to Pearson correlation analysis, was preferred to account for nonlinear relationships, with r indicating the correlation coefficient (PAST software, Hammer et al, 2001).The analyses were conducted on daily (Table 3A) and monthly (Table 3B) time scales. The Bonferroni test was applied to prevent data from spuriously appearing as statistically significant by making an adjustment during comparison testing. Additionally, to integrate both air temperature and rainfall amount effects, a multiple regression model for $\delta^{18}O$ was carried out using PAST software for every studied site (Table 3C).

3.5. Backward-trajectory and moisture uptake analysis

Backward-trajectory analysis was performed using the Hybrid Single-Particle Lagrangian Integrated Trajectory (HYSPLIT) Model (Version 4.8) (Draxler and Rolph, 2010) and following a similar methodology to Baldini et al. (2010) over a 24 hours lifetime (120 hours trajectories were also calculated, Fig. S1) for three of the seven stations: Oviedo, Borrastre and Mallorca. Global Data Assimilation System (GDAS) have been used in Hysplit simulations with 0.5ºx0.5º spatial resolution. Thus, to facilitate the statistical comparison of mean trajectory paths and moisture uptake regions with the oxygen isotope signature of sampled rain events, the vector angle between every site (Oviedo-Borrastre-Mallorca) and each hourly position along 24-h back trajectories (at 700 and 850 hPa) for each event was estimated, following the methodology presented in Baldini et al. (2010). Once all the vectors that represent the mean trajectory of the air mass transport associated with precipitation were produced for each sampled event, they were averaged and presented in a compass rose using 10° intervals, together with $\delta^{18}O_p$ values and rainfall amount of each daily sample (mm) provided by weather stations close to each analyzed location. To explore the moisture uptake along the backwards trajectories, we have performed a new analysis in all events (850hpa trajectories) using Baldini's method (Baldini et al., 2010) in a more restrictive way (see also Iglesias González, 2019), to identify the locations where moisture uptake processes have taken place during the 48h before the rainfall samples were collected. Taking into account that the Iberian Peninsula is surrounded by ocean, together with the fact that most of the analyzed rainfall events were produced by frontal systems and convection events (see synoptic analysis), only 850-hPa air mass moisture uptake events have been considered as relevant to our new analysis. In addition, while Baldini et al, (2010) considered moisture uptake processes with an increase of 0.1 g H_2O_v/kg_{air} in one hour as significant, in our analysis we only took into account events in which moisture uptake process where higher than 0.25 g H_2O_v/kg_{air}; therefore, if there exists any influence on the rainfall isotopic signal, it would be easier to identify than in previous studies. With this restricted method, and considering all the events examined, more than 3000 moisture uptake events have been identified. These events were analyzed considering seasonal variability and the different locations where the rainfall samples were collected (Oviedo, Borrastre, Mallorca).

3.6. Precipitation types

Lastly, to better explore the role of the type of precipitation in controlling the isotopic composition of rainfall across northern Iberia, we applied a disaggregation procedure of the precipitation series on the basis of their meteorological origin, following the same subjective criteria described in Millan et al. (2005) (see disaggregation criteria in his Table 1). This method classifies each precipitation event on the basis of its characteristics and moisture source region, distinguishing between three categories (Figure 1B, Table 4): (i) frontal systems associated with passing cold fronts from the west, (ii) convective-orographic storms driven by differential heating, sea breezes and local winds (Azorin-Molina et al., 2009) and (iii) easterly advection from the Mediterranean Sea (backdoor cold fronts). The Kruskal-Wallis H test (sometimes also called the "one-way ANOVA on ranks") is a rank-based nonparametric test (Hammer et al., 2001) that was applied to the three rainfall categories to determine if there were statistically significant differences in their $\delta^{18}O_p$ distributions (Table 5).

4 Results and discussion

This section is focused on characterizing $\delta^{18}O_p$ in the studied transect in northern Spain on daily and monthly time scales and on analysing the main factors behind the observed patterns. It is important to highlight here the high complexity of the hydrological cycle, with many processes playing a role in the formation of the isotope signals in precipitation, ranging from source processes, transport processes, as well as cloud and rainfall formation at the sampling site. Those factors may also overlap, making it difficult to disentangle their effects. The following sections are presented as follows: Sect. 4.1 and 4.2 are dedicated to daily and monthly data respectively. Sect 4.3 is dedicated to the influence of geographical parameters, such as distance from coast or elevation of the studied sites. Sect. 4.4 deals with the role of meteorological parameters, in particular, local air temperature and precipitation amount. Sect. 4.5 investigates the role of moisture origin on $\delta^{18}O_p$ variability while Sect. 4.6 explores the role of rainfall type (convective, frontal) in determining $\delta^{18}O_p$.

4.1 Daily rainfall isotopic variability

The rainfall samples for the studied stations on a daily scale define local meteoric water lines (LMWL) that are roughly parallel for all sites with similar offset from the Global Meteoric Water Line (GMWL, $\delta^2H = 8*\delta^{18}O + 10$) (Figure 2). All the slopes and the intercepts are lower than the GMWL, with slopes ranging from 6.9 to 7.2 and intercepts from 1.05 to 6.4 (Figure 2). Thus, the LMWLs determined from daily data for each of the studied sites reveal a broadly similar regional signal and are consistent with previous studies using GNIP data from southern France (Genty et al., 2014), even though that study is based on monthly $\delta^{18}O_p$ data. The slopes obtained in our study are slightly lower compared to a previous analysis in the IP (Araguás-Araguás and Diaz Teijeiro, 2005), in which the sampling period only covered the rainy season (October to March).
Despite the differential time coverage of samples among the studied stations, the different daily time series of $\delta^{18}O_p$ at all stations are presented together (Figure 3). Figures with $\delta^{18}O_{p,}$ d-excess and total precipitation for every separate site are included as Supplementary material (Figs. S2 to S8). From 2010 to 2017, daily $\delta^{18}O_p$ clearly show lower values in winter and higher (sometimes positive) values in summer at all stations (Figure 3). Yet some summer rainy episodes (e.g., the 25 June 2014 event in Borrastre or the 18 June 2016 one in Barcelona) exhibit values typical of winter after several days of rain or after an intense rainfall event (41.6 mm in Borrastre from 23rd to 25th June, or 17.8 mm in Barcelona from the 17th to 18th June). Also evident in Figure 3 is the synchronicity among stations for specific events. A good example is the episode of 16-18th November 2013 (inset in Figure 3) when very negative values were reached at Molinos (black line), Borrastre (green line) and Mallorca (red line). This period was characterized by intense widespread rain – eg. 43 mm in Mallorca and 36 mm in Molinos (Table S1). At the three sites, this period was among the rainiest in our record with some of the lowest $\delta^{18}O_p$ values recorded.
It is evident from this large dataset that there is significant day-to-day variability, as large as the seasonal cycle, thus emphasising the need for high-resolution measurements such as the ones presented in this study to characterize rainfall isotopic variability in northern Iberia.

4.2 Monthly rainfall isotopic variability

Seasonality in $\delta^{18}O_p$ in northern Iberia is further explored in Figure 4 (data in Table 2, Table S2). All stations exhibit a clear seasonal pattern in air temperature, with a peak in July/August and minimum values in December/January and a similar seasonal signal in $\delta^{18}O_p$ with peak $\delta^{18}O_p$ values in summer and minimum $\delta^{18}O_p$ in winter. It is worth noting that precipitation exhibits a bi-modal pattern with peaks in spring and autumn, which is not reflected in $\delta^{18}O_p$. The average seasonal differences between the $\delta^{18}O_p$ maximum values in July-August and minimum values in January-February are large: 5.8‰ at Borrastre, 4.6‰ at Ortigosa de Cameros, 6.2‰ at Molinos and about 4‰ at Mallorca-Barcelona. Interestingly, the Oviedo-El Pindal samples reveal a very different pattern, with a marked reduction in seasonality compared to the other sites (2 ‰ $\delta^{18}O_p$ difference between winter and summer) (Figure 4B). The seasonal difference from winter to summer in Oviedo-El Pindal is similar to the values published by Genty et al., (2014) for stations in southern France (e. g., 2.1 ‰ in Villars with only Atlantic influence, and 3.6 ‰ in Orgnac with Atlantic and Mediterranean influence). The weak seasonality in the Oviedo-El Pindal $\delta^{18}O_p$ signal and the similarity to the Villars station could be related to the origin and type of precipitation (Sect. 4.5 and 4.6). Even though there are fewer precipitation events associated with fronts in summer than in winter, Oviedo and Villars stations are characterized by a relatively constant source of precipitation throughout the year associated with Atlantic fronts and an absence of a dry season (Figure 4A). This is in clear contrast to the other stations, which are characterized by a more hybrid Atlantic/Mediterranean climate (e.g., Orgnac, Genty et al., 2014). In particular, in Barcelona and Mallorca the seasonal difference in $\delta^{18}O_p$ monthly values is high (6‰) (Figure 4B). At these two stations, the influence of different air mass histories may be important to explain the observed high variability. These influences are further evaluated using back trajectory and moisture uptake analysis in Sect. 4.5.

4.3 Geographical controls on rainfall isotopic variability

The combination of the various isotope effects results in consistent and spatially coherent variations in $\delta^{18}O_p$ values, that are primarily related to geographical location and regional orography (Rozanski et al., 1993; Bowen, 2008), parameters that influence the circulation and therefore the air mass history. Preliminary observation of the monthly averaged $\delta^{18}O_p$ data (Table 2 and Figure 4B) reveals similar values among the sites located at opposite ends of the transect, that is, Oviedo and El Pindal compared to Barcelona and Mallorca. This similarity was unexpected since differences in moisture source conditions at the location of the moisture uptake were anticipated to be markedly different (see also Sect. 4.5). However, this similarity may be explained by two processes, partly associated to the geographical location of the studied sites.

First, the fact that Oviedo and El Pindal rainfall samples show enriched $\delta^{18}O_p$ values is consistent with their location in the Cantabrian coast, very close to the Atlantic Ocean, with climatological oceanic conditions characterized by relatively mild temperatures (Table 1). Thus, Oviedo (and El Pindal) are the stations that receive the first precipitation produced via contact with the Atlantic; they are the stations in the transect least affected by the “continental effect”, which occurs when moist air and clouds move inland from the Atlantic Ocean and become gradually isotopically depleted due to progressive rainout

(Dansgaard, 1964). Therefore, as we follow the typical displacement of an Atlantic front on its way to the IP, from west to east, we find progressively more negative winter $\delta^{18}O_p$ values (see values for January-February-March in Table 2), going from El Pindal (-6.0‰) to Ortigosa de Cameros (-8.1‰) to Borrastre (-9.8‰) and, finally, to Molinos (-10.0‰). This pattern is not as evident in other seasons where the entrance of Atlantic fronts is not the dominant synoptic situation that generates rainfall in the transect (Rüdisühli et al., 2020). In addition to this "continental effect", which accounts for only a small gradient in $\delta^{18}O_p$ (about 0.002‰ per km in Europe as described in Rozanski et al., 1993), the higher annual mean air temperature in both Mallorca and Barcelona, on the one hand, and Oviedo and El Pindal, on the other, compared to the other stations (Table 1), may help explain their similar $\delta^{18}O_p$ values. The effect of warmer temperature on the less negative $\delta^{18}O_p$ values recorded will be discussed with more detail below (Sect. 4.4).

Second, another geographical factor that could account for the similarities found in stations at opposed ends of the transect is related to the elevation at those sites. Ortigosa de Cameros, Molinos and Borrastre stations, the three stations located at a higher elevation, show monthly $\delta^{18}O_p$ values quite similar and, normally, more negative than Oviedo, El Pindal, Barcelona and Mallorca sites, which are close to sea-level. This pattern is particularly clear for autumn values (see monthly averaged $\delta^{18}O_p$ values from September to December in Table2 along the west-to-east transect). Therefore, the "elevation effect" (Siegenthaler and Oeschger, 1980) likely also plays a role in explaining the similarities among coastal sites. Considering the $\delta^{18}O_p$ annual averages (Table 2), there is a difference of 2.3‰ between Molinos (1040 m asl) and Mallorca (90 m asl). Based on the difference of elevation, the vertical isotopic gradient observed is -0.24‰ per 100 m of elevation. This result is consistent with previous studies in other mountain ranges such as the Alps, where an altitudinal gradient of -0.2 to - 0.3‰ per 100 m of elevation was observed (Ambach et al., 1968; Siegenthaler and Oeschger, 1980).

In the next sections we explore how the geographical factors reviewed in this section (distance to the coast or continental effect and elevation effect) exert a direct influence on the observed spatial distribution of rainfall $\delta^{18}O_p$ by their influence on other controlling factors: air temperature, rainfall amount, air mass origin and rainfall type.

4.4 The influence of air temperature and rain amount on the spatial distribution of rainfall $\delta^{18}O_p$ values

Spearman's rank correlation analysis (Table 3) reveals that $\delta^{18}O_p$ does not correlate with air temperature or amount of precipitation in a similar way at each station, neither at daily nor monthly time scales, thus reinforcing the need for conducting calibrating studies on a local basis, particularly when conducting palaeoclimatic reconstructions (Leng, 2006). Air temperature appears as the variable better correlated with $\delta^{18}O_p$ across the west-to-east transect, with modest but statistically significant correlations (daily scale) at all sites (red numbers in Table 3A) except Oviedo and Barcelona, most likely due to the low number of daily samples (n=39 and n=53, respectively). The coefficient of correlation among $\delta^{18}O_p$ daily values and air temperature is highly variably from west to east: El Pindal ($r_s = 0.34$; $p = 0.001$), Ortigosa de Cameros ($r_s = 0.25$; $p = 0.001$), Molinos ($r_s = 0.42$; $p < 0.001$), Borrastre ($r_s = 0.29$; $p < 0.01$) and Mallorca ($r_s = 0.35$; $p = 0.001$)

(Table 3A). Regarding monthly values, air temperature is significantly correlated with $\delta^{18}O_p$ values at eastern stations, with the highest coefficients associated with higher altitude sites (e.g., in Molinos with $r_s = 0.76$ and $p<0.001$ or in Borrastre with $r_s = 0.61$ and $p<0.001$) (Table 3B).

The influence of rainfall amount on $\delta^{18}O_p$ is strong in tropical regions where deep convection is frequent, although it may also occur in the extratropics in summer (Bar-Matthews et al., 2003; Treble et al., 2005b). Correlation among rainfall amount and $\delta^{18}O_p$ is negative, associated to the raindrop evaporation during periods of sparse rains (Dansgaard, 1964; Risi et al., 2008) when the relative humidity is low and is thus not a purely equilibrium process. In the studied transect, at the daily scale, the strongest correlation is observed in Barcelona (r_s = -0.35; p=0.029) (Table 3A). There is also a significant correlation at the two sites of the Iberian Range (r_s = -0.32; p=1.05E-05 in Ortigosa and r_s = -0.19; p=0.005 in Molinos). Interestingly, the westernmost stations (El Pindal and Oviedo) do not show a significant $\delta^{18}O_p$–precipitation correlation on daily or monthly scales. This lack of a correlation in the Atlantic sites contrasts with a previous study carried out in northern Spain at a site also characterized by an Atlantic climate (Matienzo depression), where a significant $\delta^{18}O_p$–precipitation monthly correlation was found (r = -0.51; p < 0.01) (Smith et al., 2016). In our study, the $\delta^{18}O_p$–precipitation correlation at monthly scale is only significant in Molinos, in the Iberian Range (r_s = - 0.4; p=0.018), while no correlation is observed at the other sites (Table 3B).

To further assess the relative role of temperature and rainfall amount effects, a multiple regression model for $\delta^{18}O_p$ was carried out for the seven studied sites (Table 3C). The dependence of $\delta^{18}O_p$ on air temperature has been extensively studied, yielding an *average* slope for mid-latitude continental stations of 0.58‰/°C (Rozanski et al., 1993). In our data that value is highly variable in time and space. The strongest air temperature-$\delta^{18}O_p$ relationship, based on daily data, are found at Borrastre (0.4‰/°C), Molinos (0.4‰/°C) and Barcelona (0.37‰/°C) while the weakest at Oviedo/El Pindal (0.2‰/°C). The other three stations, Ortigosa de Cameros (0.25‰/°C) and Mallorca (0.317‰/°C), show intermediate values. Compared to other areas, such as the Alps with temperature-$\delta^{18}O_p$ gradients of 0.5 to 0.7 ‰ per °C, the results presented above indicate that, although important, air temperature only explains part of the observed $\delta^{18}O_p$ variability and is, therefore, not the only control. Air temperature, together with amount of precipitation (Table 3C), account for less than 40 % of the variability of $\delta^{18}O_p$ in the study transect. Since the origin of air masses producing rainfall and the type of rainfall (i.e., convective vs. frontal) is also spatially dependent in northern Iberia, these variables and their influence on the observed $\delta^{18}O_p$ variability are investigated in Sect. 4.5 and 4.6 below.

4.5 The role of the *source effect* in modulating northern Iberian Peninsula $\delta^{18}O_p$

The source effect describes how air masses derived from different moisture sources have distinct $\delta^{18}O_p$ values (e.g., Friedman, 2002). The source effect results from varying air mass histories, different conditions of the moisture source (air temperature, relative humidity and wind speed) and regional differences in the $\delta^{18}O$ of the surface ocean (LeGrande and

Schmidt, 2006). In the case of northern IP, it is necessary to consider the effect of both the Atlantic Ocean and Mediterranean Sea as important sources of atmospheric moisture (Gimeno et al., 2010). Typical present-day $\delta^{18}O$ values of seawater (LeGrande and Schmidt, 2006) indicate slightly different values for the Atlantic Ocean and the Mediterranean Sea, due to temperature and salinity differences. Source $\delta^{18}O$ values range from 1 to 1.5‰ in the subtropical Atlantic to 2‰ in the Mediterranean (Schmidt et al., 1999). These differences in the source (about 0.5 - 1 ‰) are small, but they are further modulated by the air mass history, thus resulting in a change in the relative influence of moisture sources on $\delta^{18}O_p$ along the west-to-east transect.

To evaluate the role of air mass origin in determining $\delta^{18}O_p$ values at a daily scale in northern Iberia and Balearic islands, back trajectories were calculated for all the rainy days and subsequently averaged into wind rose diagrams, following the representation used in previous studies (Smith et al., 2016), for three stations along our northern Iberia transect: Oviedo and Mallorca, the two extreme locations, and Borrastre, located at an intermediate location, comprising a total number of 519 events. This analysis reveals the dominance of western trajectories at the three studied sites considering 24h life-time, with very few episodes associated with a different direction (Figure 5, see also Fig. S1 for trajectories calculated over a 120h lifetime). In fact, comparison with the analysis carried out over 24h and over 120h shows only few episodes with trajectories from the SW (e.g., Borrastre) or SE (e.g., Mallorca) and, interestingly, they all have different $\delta^{18}O_p$ values (see below).

Despite the three sites sharing a common dominant WNW direction of Atlantic air mass origin, they behave quite differently in terms of amount of rainfall and $\delta^{18}O_p$ values for every event. Oviedo (with a temperate oceanic climate - Cfb, Table 1) presents a narrower range in both rainfall amount and $\delta^{18}O_p$ in comparison to the other two sites (clearly seen at 120h, Fig. S1), as shown by the negligible frequency of rainfall amounts above 32 mm (orange) or below 2 mm (purple), while "extreme" events are much more common in Borrastre or Mallorca sites. Similarly, in figure 5B, where the isotopic values for the different trajectories are plotted, Oviedo appears as the station with more uniform $\delta^{18}O_p$ values (between -10 and -2‰) compared to the other two stations. Thus, in Borrastre and Mallorca, $\delta^{18}O_p$ values between -8 and -12‰ (red – green – yellow - dark blue) are only present in northwestern trajectories, while less negative values (- 6 to 2‰) appear in events with a SW and SE directions (see also Fig. S1). These results confirm the homogeneity of the Atlantic sites in terms of $\delta^{18}O_p$ amplitude (Cantabrian coastal sites: Oviedo, El Pindal) compared to the intermediate (Iberian range and Pyrenean sites: Ortigosa de Cameros, Molinos and Borrastre) stations already described by monthly data in Figure 4.

This study of the source origin indicates a low, almost negligible, presence of trajectories associated with Mediterranean air mass advections. However, it is well-known that, since meteorological processes connected to convection (e.g., orographic, dynamic and thermodynamic) can produce moisture uptake in less than 6h (Romero et al., 2000, 1997; Tudurí and Ramis, 1997) they will not be well-captured in back trajectory analyses that are computed for the previous 24 hours (and even less for 120h, Fig.S1). Therefore, it is important to note that this method provides information on the air mass origin (source effect) but not on the moisture uptake regions. In that way, the dominant WNW air mass origin for the three studied stations is clear.

To account for the different moisture uptake processes along the studied trajectories, we followed Baldini et al. (2010) methodology in a more restricted way (see Methods) for Oviedo-Borrastre-Mallorca stations (Figure 6). Our findings highlight the importance of moisture uptake in generating the observed $\delta^{18}O_p$ differences along our west-to-east transect, with Oviedo and Mallorca showing a clearly dominant marine signal (Atlantic and Mediterranean, respectively), while in Borrastre the moisture uptake occurs over the whole Iberian Peninsula with the marine uptake being less important. The Oviedo station appears very homogenous in terms of the moisture uptake regions, clearly concentrated on the Portuguese margin and with very few events characterized by recycled continental moisture. Interestingly, we observe seasonal differences in the dominant regions for moisture uptake, particularly at Borrastre station. Thus, the contribution of continental moisture recycling, although observed along the whole year, is more frequent in summer, as deduced from the red dots located very close to the station, pointing to local convective processes (Figure 6). The oceanic contribution to Borrastre rainfall is small and present mostly in winter (WNW oceanic source) and, to a lesser extent, spring and autumn (Mediterranean source). A recent study analyzing the trace element composition of precipitation also shows this seasonal tendency for the Pyrenees (Suess et al., 2020). This seasonality in land vs. ocean moisture source contribution to Pyrenean precipitation is most certainly an important driver of the seasonal cycle of the isotope signals in precipitation, as was previously highlighted in many stations in Figure 4B. The moisture uptake regions identified for Mallorca rainfall events are also quite heterogeneous, highlighting the Mediterranean as the dominant source for moisture uptake, while in winter-spring some events are observed to originate in the WNW sector. Additionally, some southern events arriving from North Africa are also detected, indicating the importance of that area to account for the Balearic islands rainfall composition. In addition, we suggest that Borrastre station offers a good representation of the Iberian rainfall in terms of $\delta^{18}O_p$ composition since it receives moisture from a wide area, thus being of utility for further paleoclimatic studies in the Pyrenean region. Similarly, Oviedo site appears to be a good prototype for the Atlantic region, allowing nearby palaeoclimate sites to be compared with well-known marine cores from the Portuguese margin. Finally, Mallorca site would represent the Western Mediterranean in terms of preferred moisture uptake region.

4.6 The influence of rainfall type on isotopes.

The influence of rainfall type on $\delta^{18}O_p$ is well documented globally, with different $\delta^{18}O_p$ observed depending on the type of precipitation: convective showers, frontal, continuous stratiform precipitation, etc. (Aggarwal et al., 2012). This dependency is observed in previous studies both on daily or monthly timescales (Aggarwal et al., 2016), with few examples of frontal precipitation (Aemisegger et al., 2015) or tropical convective processes (Risi et al., 2008) in Europe. These previous studies indicated that $\delta^{18}O_p$ values were lower when precipitation was dominantly stratiform and higher when it was mostly convective. The main reason to explain this difference lies on the processes of condensation associated with boundary layer moisture which produce higher isotope ratios in convective rain (Aggarwal et al., 2016). Additionally, some studies in the

Mediterranean region also directly link the isotopic signature of the precipitation to the prevailing weather conditions during the rainfall event (Celle-Jeanton et al., 2001), helping to further understand the role of water vapour transport and the moisture cycling during convective events (Lee et al., 2019).

Here we explore how the specific synoptic situation, i.e., rainfall types or rainfall components, influence $\delta^{18}O_p$ values across the studied transect. Table 4 shows the percentage of rain events associated with each type of precipitation, which were previously defined following (Millán et al., 2005) and represented in Figure 1B: (i) Atlantic frontal systems (westerly winds), (ii) convective–orographic storms, and (iii) backdoor cold fronts from the Mediterranean Sea (easterly winds)..

The prominence of rainfall associated with Atlantic fronts is evident (above 40% in the seven studied stations). This percentage decreases eastward, from 68 /71% in Oviedo/El Pindal to 58 /41 % in Barcelona/Mallorca. A previous study at a north Iberian site (Matienzo, Cantabria) indicates that approximately 80% of air masses originate in the North Atlantic and that their movement is associated with westerly frontal systems (Smith et al., 2016). This situation appears to be true for the Cantabrian coastal sites; for the Mediterranean and Iberian Range sites, however, the Atlantic and Mediterranean sources are of comparable importance (including backdoor cold fronts) (Table 4). Distance to the Mediterranean and elevation are also important factors in determining the frequency of rainfall associated with backdoor cold fronts. Thus, backdoor cold fronts are associated with 39% of Mallorca rain events and are still frequent situations at the two sites from the Iberian Range (21% in Ortigosa de Cameros and 24% in Molinos). The frequency of convective precipitation is higher at the three mountain sites (21% in Ortigosa de Cameros, 24% in Molinos and 23% in Borrastre), compared to those sites at lower elevation (17% in Oviedo; 12% in El Pindal, 17% in Barcelona and 20% in Mallorca).

The Kruskal-Wallis test was applied to investigate if there were significant differences in the $\delta^{18}O_p$ values of the three rainfall types analysed (Atlantic, backdoor frontal precipitation, and convective) in the studied stations at the daily scale. Test values shown in Table 5 (p values < 0.05) indicate the $\delta^{18}O_p$ values of at least two of the three rainfall types are significantly different (this does not apply to Oviedo and Barcelona since the number of freedom degrees is too small to yield a significant result). We conclude that the type of rainfall (frontal versus convective) is an important factor controlling $\delta^{18}O_p$ values in the studied transect at the daily scale. This result is also evident where the three rainfall types are represented according to their $\delta^{18}O_p$ composition (Figure 7). Thus, regarding $\delta^{18}O_p$ composition, convective precipitation (in green in Figure 7) is associated with the highest $\delta^{18}O_p$ values, while events related to Atlantic and backdoor cold fronts display more negative $\delta^{18}O_p$ values (albeit with a large spread), consistent with previous studies (Aggarwal et al., 2016). The highest $\delta^{18}O_p$ values associated with convective precipitation may be related to the critical role played by the re-evaporation of droplets, a process that usually takes place during convective rainfall (Bony et al., 2008). In any case, what is relevant here is the similarity between $\delta^{18}O_p$ values associated with the two types of frontal rains (Atlantic fronts and Mediterranean backdoor cold fronts), while there is a significant difference when considering the type of precipitation, i.e. convective versus frontal.

5 Conclusion

The major findings in this study are summarized as follows:

- The analysis of $\delta^{18}O_p$ and δ^2H_p at seven stations along a west-to-east transect in northern Iberia and Balearic Islands yields similar LMWLs, but all with lower slope and intercept values than the GMWL.
- Oviedo/El Pindal and Mallorca/Barcelona rainfall samples display the least negative $\delta^{18}O_p$ and δ^2H_p values in the transect. Our results suggest that this similarity between the two stations located at the western and eastern ends of the northern IP is due, firstly, to the initial condensate of water vapour generated over the North Atlantic and, secondly, to the influence of air masses originating in the Mediterranean Sea, together with the much warmer temperatures there than in the other three sites. Besides those effects, the "elevation effect" must be taken into account to explain the more negative average values at the three mid-transect stations (Ortigosa de Cameros, Borrastre and Molinos).
- The seasonal variability is larger at Ortigosa de Cameros, Borrastre and Molinos, while it is reduced in Oviedo-El Pindal due to the single origin of rainfall in that area and the concentrated regions of moisture uptake along the Portuguese margin.
- Air temperature appears to be the best correlated variable with $\delta^{18}O_p$ on daily and monthly time scales, with the highest air temperature-$\delta^{18}O_p$ dependency found at the Pyrenean station (slope of 0.38‰/°C). Only a few sites in the transect show a significant negative correlation with precipitation amount (monthly in Molinos; daily in Ortigosa de Cameros, Molinos, Barcelona and Mallorca).
- The dominance of rainfall with an Atlantic origin is clear in the study of rainfall back trajectories associated with each rainy event in Oviedo, Borrastre and Mallorca sites, but the regions in which moisture uptake takes place are highly heterogeneous in space and time. At Borrastre station, moisture comes from all over the Iberian Peninsula, with a dominance of recycled continental moisture and less influence of oceanic moisture in summer (Atlantic influence in winter, Mediterranean influence in spring and autumn).
- Convective rainfall yields higher $\delta^{18}O_p$ values, while rainfall events related to Atlantic and backdoor fronts exhibit more negative $\delta^{18}O_p$ values.

In conclusion, the northern Iberian region is under the influence of two climatic regimes (Atlantic and Mediterranean) and affected by different moisture source origins and uptake regions. Therefore, the synoptic-scale atmospheric circulation is playing a key role in determining the ranges, values and seasonal distribution of $\delta^{18}O_p$ variability.

Data availability

All data are included in the Supplementary Tables S1 and S2.

Author contribution

The paper was conceived by AM, CPM, MB, CS, HS and IC. MI carried out the back trajectory and moisture uptake studies and CAM provided the synoptic patterns during rainfall days. JF, CO, ArM and ADH contributed to rainfall sampling and/or isotopic analyses. IB and FV helped with data interpretation. All authors contributed to the writing of the paper.

Competing interests

The authors declare that they have no conflict of interest

Acknowledgements

We acknowledge CTM2013-48639-C2-2-R (OPERA), CGL2016-77479-R (SPYRIT) and PID2019-106050RB-100 (PYCACHU) projects for main funding. Part of the previous isotopic analyses were carried out in the framework of GA-LC-030/2011, CGL2010-16376 and CGL2009-10455/BTE projects. This work is a contribution of Geomorfología y Cambio Global, Geotransfer and PaleoQ (IUCA) research groups (Aragón Government). We are extremely grateful to all people who carried out the rainfall sampling: Emilio (Molinos, Teruel); Ramiro Moreno (Borrastre, Huesca); M. Angeles, Sara and Juan (Ortigosa de Cameros, La Rioja); Montse Guart (Barcelona); Alejandro Gallardo and Joan Fornós (Manacor, Mallorca). The Ebro Hydrographic Confederation network (SAIH www.saihebro.com) and the NOAA database are acknowledged for providing, respectively, meteorological data and software for the back trajectory analyses (HYSPLIT). We thank Georgina Mateu of the University of Barcelona for their temperature and precipitation data. We also acknowledge the www.meteo4u.com, www.meteoclimatic.net, http://www.larioja.org/emergencias-112/es/meteorologia and http://balearsmeteo.com websites and the Sant Llorenç des Cardassar observatory for the meteorological data in this region and the European Centre for Medium-Range Weather Forecasts for the ERA-Interim dataset. IC also thanks the ICREA Academia program from the Generalitat de Catalunya. We dedicate this study to our colleague Carlos Sancho who intensively worked to produce this large $\delta^{18}O$ rainfall dataset for northern Iberia and to Ramiro Moreno who collected rainfall samples and meteorological data in Borrastre village for eleven years. Both passed away, in February 2019 and April 2020 respectively.

References

AEMET, Instituto de Meteorologia de Portugal, 2011. Atlas climático Ibérico. Temperatura del aire y precipitación (1971-2000).

Aemisegger, F., Spiegel, J.K., Pfahl, S., Sodemann, H., Eugster, W., Wernli, H., 2015. Isotope meteorology of cold front passages: A case study combining observations and modeling. Geophysical Research Letters 42, 5652–5660. https://doi.org/10.1002/2015GL063988

Aggarwal, Alduchov Oleg A., Froehlich Klaus O., Araguas-Araguas Luis J., Sturchio Neil C., Kurita Naoyuki, 2012. Stable isotopes in global precipitation: A unified interpretation based on atmospheric moisture residence time. Geophysical Research Letters 39. https://doi.org/10.1029/2012GL051937

Aggarwal, P.K., Romatschke, U., Araguas-Araguas, L., Belachew, D., Longstaffe, F.J., Berg, P., Schumacher, C., Funk, A., 2016. Proportions of convective and stratiform precipitation revealed in water isotope ratios. Nature Geoscience 9, 624–629. https://doi.org/10.1038/ngeo2739

Ambach, W., Dansgaard, W., Eisner, H., Møller, J., 1968. The altitude effect on the isotopic composition of precipitation and glacier ice in the Alps. Tellus 20, 595–600. https://doi.org/10.3402/tellusa.v20i4.10040

Araguás-Araguás, L.J., Diaz Teijeiro, M.F., 2005. Isotope composition of precipitation and water vapour in the Iberian Peninsula, in: Isotopic Composition of Precipitation in the Mediterranean Basin in Relation to Air Circulation Patterns and Climate. Vienna, Austria, pp. 173–191.

Archer, C.L., Caldeira, K., 2008. Historical trends in the jet streams. Geophys. Res. Lett. 35, L08803. https://doi.org/10.1029/2008GL033614

Azorin-Molina, C., Chen, D., Tijm, S., Baldi, M., 2011. A multi-year study of sea breezes in a Mediterranean coastal site: Alicante (Spain). International Journal of Climatology 31, 468–486. https://doi.org/10.1002/joc.2064

Azorin-Molina, C., Connell, B.H., Baena-Calatrava, R., 2009. Sea-Breeze Convergence Zones from AVHRR over the Iberian Mediterranean Area and the Isle of Mallorca, Spain. J. Appl. Meteor. Climatol. 48, 2069–2085. https://doi.org/10.1175/2009JAMC2141.1

Baldini, L.M., McDermott, F., Baldini, J.U.L., Fischer, M.J., Möllhoff, M., 2010. An investigation of the controls on Irish precipitation δ18O values on monthly and event timescales. Clim Dyn 35, 977–993. https://doi.org/10.1007/s00382-010-0774-6

Bar-Matthews, M., Ayalon, A., Gilmour, M.A., Matthews, A., Hawkesworth, C.J., 2003. Sea-land oxygen isotopic relationships from planktonic foraminifera and speleothems in the Eastern Mediterranean region and their implication for paleorainfall during interglacial intervals. Geochimica et Cosmochimica Acta 67, 3181–3199.

Bartolomé, M., Moreno, A., Sancho, C., Stoll, H.M., Cacho, I., Spötl, C., Belmonte, Á., Edwards, R.L., Cheng, H., Hellstrom, J.C., 2015. Hydrological change in Southern Europe responding to increasing North Atlantic overturning during Greenland Stadial 1. PNAS 112, 6568–6572. https://doi.org/10.1073/pnas.1503990112

Berrisford, P., Dee, D.P., Fielding, M., Fuentes, M., Kallberg, P.W., Kobayashi, S., Uppala, S., 2009. The ERA-Interim archive (No. 1), ERA Report Series,. ECMWF.

Bony, S., Risi, C., Vimeux, F., 2008. Influence of convective processes on the isotopic composition (δ18O and δD) of precipitation and water vapor in the tropics: 1. Radiative-convective equilibrium and Tropical Ocean–Global Atmosphere–Coupled Ocean-Atmosphere Response Experiment (TOGA-COARE) simulations. Journal of Geophysical Research: Atmospheres 113. https://doi.org/10.1029/2008JD009942

Bowen, G.J., 2008. Spatial analysis of the intra-annual variation of precipitation isotope ratios and its climatological corollaries. Journal of Geophysical Research 113. https://doi.org/10.1029/2007JD009295

Coleman, M.L., Shepherd, T.J., Durham, J.J., Rouse, J.E., Moore, G.R., 1982. Reduction of water with zinc for hydrogen isotope analysis. Anal. Chem. 54, 993–995. https://doi.org/10.1021/ac00243a035

Craig, H., 1961. Isotopic Variations in Meteoric Waters. Science 133, 1702–1703. https://doi.org/10.1126/science.133.3465.1702

Dansgaard, W., 1964. Stable isotopes in precipitation. Tellus 16, 436–468. https://doi.org/10.1111/j.2153-3490.1964.tb00181.x

Dee, D.P., Uppala, S.M., Simmons, A.J., Berrisford, P., Poli, P., Kobayashi, S., Andrae, U., Balmaseda, M.A., Balsamo, G., Bauer, P., Bechtold, P., Beljaars, A.C.M., Berg, L. van de, Bidlot, J., Bormann, N., Delsol, C., Dragani, R., Fuentes, M., Geer, A.J., Haimberger, L., Healy, S.B., Hersbach, H., Hólm, E.V., Isaksen, L., Kållberg, P., Köhler, M., Matricardi, M., McNally, A.P., Monge-Sanz, B.M., Morcrette, J.-J., Park, B.-K., Peubey, C., Rosnay, P. de, Tavolato, C., Thépaut, J.-N., Vitart, F., 2011. The ERA-Interim reanalysis: configuration and performance of the data assimilation system. Quarterly Journal of the Royal Meteorological Society 137, 553–597. https://doi.org/10.1002/qj.828

Díaz, M.F., Rodríguez, J., Pérez, E., Castaño, S., Araguás, L., 2007. Factors controlling the stable isotopic composition of recent precipitation in Spain, in: Advances in Isotope Hydrology and Its Role in Sustainable Water Resources Management (IHS-2007). Proceedings Series. Proceedings of an International Symposium on Advances in Isotope Hydrology and Its Role in Sustainable Water Resources Management (IHS-2007). pp. 239–249.

Díaz-Tejeiro, M.F., Pérez-Zabaleta, E., Prado-Pérez, A., Bardasano-Picazo, L., Muñoz-Delavarga, D., Rodríguez, J., 2013. La Red Española de Vigilancia de Isótopos en la Precipitación (REVIP). Presented at the XI CONGRESO NACIONAL DE GEOQUÍMICA, Soria.

Domínguez-Villar, D., Wang, X., Krklec, K., Cheng, H., Edwards, R.L., 2017. The control of the tropical North Atlantic on Holocene millennial climate oscillations. Geology 45, 303–306. https://doi.org/10.1130/G38573.1

Draxler, R.R., Rolph, G.D., 2010. HYSPLIT (HYbrid Single-Particle Lagrangian Integrated Trajectory) Model access via NOAA ARL READY Website. http://ready.arl.noaa.gov/HYSPLIT.php.

Epstein, S., Mayeda, T., 1953. Variation of O18 content of waters from natural sources. Geochimica et Cosmochimica Acta 4, 213–224. https://doi.org/10.1016/0016-7037(53)90051-9

Field, R.D., 2010. Observed and modeled controls on precipitation δ^{18}O over Europe: From local temperature to the Northern Annular Mode. Journal of Geophysical Research 115. https://doi.org/10.1029/2009JD013370

Fischer, B.M.C., Aemisegger, F., Graf, P., Sodemann, H., Seibert, J., 2019. Assessing the Sampling Quality of a Low-Tech Low-Budget Volume-Based Rainfall Sampler for Stable Isotope Analysis. Front. Earth Sci. 7. https://doi.org/10.3389/feart.2019.00244

Fischer, M., Baldini, L., 2011. A climate-isotope regression model with seasonally-varying and time-integrated relationships. Climate Dynamics 37, 2235–2251. https://doi.org/10.1007/s00382-011-1009-1

Friedman, I., 2002. Stable isotope composition of waters in the Great Basin, United States 1. Air-mass trajectories. Journal of Geophysical Research 107. https://doi.org/10.1029/2001JD000565

G. A. Schmidt, G. R. Bigg, E. J. Rohling, 1999. Global Seawater Oxygen-18 Database - v1.22. Global Seawater Oxygen-18 Database - v1.22. URL https://data.giss.nasa.gov/o18data/

Genty, D., Labuhn, I., Hoffmann, G., Danis, P.A., Mestre, O., Bourges, F., Wainer, K., Massault, M., Van Exter, S., Régnier, E., Orengo, Ph., Falourd, S., Minster, B., 2014. Rainfall and cave water isotopic relationships in two South-France sites. Geochimica et Cosmochimica Acta 131, 323–343. https://doi.org/10.1016/j.gca.2014.01.043

Gimeno, L., Nieto, R., Trigo, R.M., Vicente-Serrano, S.M., Lopez-Moreno, J.I., 2010. Where does the Iberian Peninsula moisture come from? An answer based on a Lagrangian approach. Journal of Hydrometeorology.

Hammer, O., Harper, D. A. T., Ryan, P. D., 2001. PAST: Paleontological statistics software package for education and data analysis. 4(1): 9pp. Palaeontologia Electronica 4 (1), 9.

Iglesias González, M.I., 2019. Variabilidad climática del noroeste de la península ibérica durante los últimos 1500 años, descrita por espeleotemas de diversas cuevas del principado de Asturias (http://purl.org/dc/dcmitype/Text). Universidad de Oviedo.

Jeelani, G., Deshpande, R.D., Galkowski, M., Rozanski, K., 2018. Isotopic composition of daily precipitation along the southern foothills of the Himalayas: impact of marine and continental sources of atmospheric moisture. Atmospheric Chemistry and Physics 18, 8789–8805. https://doi.org/10.5194/acp-18-8789-2018

Kawale, J., Chatterjee, S., Kumar, A., Liess, S., Steinbach, M., Kumar, V., 2011. Anomaly construction in climate data: issues and challenges. Proceedings of the Conference on Intelligent Data Understanding Mountain View, California, USA, 189–203.

Krklec, K., Domínguez-Villar, D., 2014. Quantification of the impact of moisture source regions on the oxygen isotope composition of precipitation over Eagle Cave, central Spain. Geochimica et Cosmochimica Acta. https://doi.org/10.1016/j.gca.2014.03.011

Lachniet, M.S., 2009. Climatic and environmental controls on speleothem oxygen-isotope values. Quaternary Science Reviews 28, 412–432.

Lee, K.-O., Aemisegger, F., Pfahl, S., Flamant, C., Lacour, J.-L., Chaboureau, J.-P., 2019. Contrasting stable water isotope signals from convective and large-scale precipitation phases of a heavy precipitation event in southern Italy during HyMeX IOP 13: a modelling perspective. Atmospheric Chemistry and Physics 19, 7487–7506. https://doi.org/10.5194/acp-19-7487-2019

LeGrande, A.N., Schmidt, G.A., 2006. Global gridded data set of the oxygen isotopic composition in seawater. Geophys. Res. Lett. 33, 5 PP. https://doi.org/200610.1029/2006GL026011

Leng, M.J., 2006. Isotopes in palaeoenvironmental research. Springer.

Llasat, M.-C., Martín, F., Barrera, A., 2007. From the concept of “Kaltlufttropfen” (cold air pool) to the cut-off low. The case of September 1971 in Spain as an example of their role in heavy rainfalls. Meteorology and Atmospheric Physics 96, 43–60. https://doi.org/10.1007/s00703-006-0220-9

López-Blanco, C., Andrews, J., Dennis, P., Miracle, M.R., Vicente, E., 2016. Sedimentary response of lake El Tobar, Spain, to climate: lake level changes after the Maunder Minimum. J. Quaternary Sci. 31, 905–918. https://doi.org/10.1002/jqs.2915

Martín-Vide, J., Olcina Cantos, J., 2001. Climas y tiempos de España. Alianza Editorial, Madrid.

Martin-Vide, J., Olcina-Cantos, J., 2001. Tiempos y climas de España.

Millán, M.M., Estrela, M.J., Miró, J., 2005. Rainfall Components: Variability and Spatial Distribution in a Mediterranean Area (Valencia Region). Journal of Climate 18, 2682–2705. https://doi.org/10.1175/JCLI3426.1

Moreno, A., Pérez-Mejías, C., Bartolomé, M., Sancho, C., Cacho, I., Stoll, H., Delgado-Huertas, A., Hellstrom, J., Edwards, R.L., Cheng, H., 2017. New speleothem data from Molinos and Ejulve caves reveal Holocene hydrological variability in northeast Iberia. Quaternary Research 1–11. https://doi.org/10.1017/qua.2017.39

Moreno, A., Sancho, C., Bartolomé, M., Oliva-Urcia, B., Delgado-Huertas, A., Estrela, M.J., Corell, D., López-Moreno, J.I., Cacho, I., 2014. Climate controls on rainfall isotopes and their effects on cave drip water and speleothem growth: the case of Molinos cave (Teruel, NE Spain). Clim Dyn 43, 221–241. https://doi.org/10.1007/s00382-014-2140-6

Pérez-Mejías, C., Moreno, A., Sancho, C., Bartolomé, M., Stoll, H., Osácar, M.C., Cacho, I., Delgado-Huertas, A., 2018. Transference of isotopic signal from rainfall to dripwaters and farmed calcite in Mediterranean semi-arid karst. Geochimica et Cosmochimica Acta 243, 66–98. https://doi.org/10.1016/j.gca.2018.09.014

Pérez-Mejías, C., Moreno, A., Sancho, C., Martín-García, R., Spötl, C., Cacho, I., Cheng, H., Edwards, R.L., 2019. Orbital-to-millennial scale climate variability during Marine Isotope Stages 5 to 3 in northeast Iberia. Quaternary Science Reviews 224, 105946. https://doi.org/10.1016/j.quascirev.2019.105946

Risi, C., Bony, S., Vimeux, F., 2008. Influence of convective processes on the isotopic composition (δ18O and δD) of precipitation and water vapor in the tropics: 2. Physical interpretation of the amount effect. Journal of Geophysical Research: Atmospheres 113. https://doi.org/10.1029/2008JD009943

Romero, R., Doswell, C.A., Ramis, C., 2000. Mesoscale Numerical Study of Two Cases of Long-Lived Quasi-Stationary Convective Systems over Eastern Spain. Mon. Wea. Rev. 128, 3731–3751. https://doi.org/10.1175/1520-0493(2001)129<3731:MNSOTC>2.0.CO;2

Romero, R., Ramis, C., Alonso, S., 1997. Numerical simulation of an extreme rainfall event in Catalonia: Role of orography and evaporation from the sea. Quarterly Journal of the Royal Meteorological Society 123, 537–559. https://doi.org/10.1002/qj.49712353902

Rozanski, K., Araguás-Araguás, L., Gonfiantini, R., 1993. Isotopic patterns in modern global precipitation. Geophysical Monograph Series 78, PP. 1-36.

Rüdisühli, S., Sprenger, M., Leutwyler, D., Schär, C., Wernli, H., 2020. Attribution of precipitation to cyclones and fronts over Europe in a kilometer-scale regional climate simulation. Weather and Climate Dynamics 1, 675–699. https://doi.org/10.5194/wcd-1-675-2020

Sancho, C., Arenas, C., Vázquez-Urbez, M., Pardo, G., Lozano, M.V., Peña-Monné, J.L., Hellstrom, J., Ortiz, J.E., Osácar, M.C., Auqué, L., Torres, T., 2015. Climatic implications of the Quaternary fluvial tufa record in the NE Iberian Peninsula over the last 500 ka. Quaternary Research 84, 398–414. https://doi.org/10.1016/j.yqres.2015.08.003

Sancho, C., Belmonte, Á., Bartolomé, M., Moreno, A., Leunda, M., López-Martínez, J., 2018. Middle-to-late Holocene palaeoenvironmental reconstruction from the A294 ice-cave record (Central Pyrenees, northern Spain). Earth and Planetary Science Letters 484, 135–144. https://doi.org/10.1016/j.epsl.2017.12.027

Siegenthaler, U., Oeschger, H., 1980. Correlation of 18O in precipitation with temperature and altitude. Nature 285, 314–317. https://doi.org/10.1038/285314a0

Smith, A., British Geological Survey, Wynn, P., Lancaster University, Barker, P., Lancaster University, Leng, M., British Geological Survey, Noble, S., British Geological Survey, Stott, A., Centre for Ecology and Hydrology, 2016. Cave monitoring and the potential for palaeoclimate reconstruction from Cueva de Asiul, Cantabria (N. Spain). International Journal of Speleology 45, 1–9. https://doi.org/10.5038/1827-806X.45.1.1928

Stoll, H., Mendez-Vicente, A., Gonzalez-Lemos, S., Moreno, A., Cacho, I., Cheng, H., Edwards, R.L., 2015. Interpretation of orbital scale variability in mid-latitude speleothem δ18O: Significance of growth rate controlled kinetic fractionation effects. Quaternary Science Reviews, Novel approaches to and new insights from speleothem-based climate reconstructions 127, 215–228. https://doi.org/10.1016/j.quascirev.2015.08.025

Suess, E., Aemisegger, F., Sonke, J.E., Sprenger, M., Wernli, H., 2019. Marine versus continental sources of iodine and selenium in rainfall at two European high-altitude locations. Environmental Science & Technology 53, 4, 1905–1917.

Treble, P.C., Budd, W.F., Hope, P.K., Rustomji, P.K., 2005a. Synoptic-scale climate patterns associated with rainfall δ18O in southern Australia. Journal of Hydrology 302, 270–282. https://doi.org/10.1016/j.jhydrol.2004.07.003

Treble, P.C., Chappell, J., Gagan, M.K., McKeegan, K.D., Harrison, T.M., 2005b. In situ measurement of seasonal δ18O variations and analysis of isotopic trends in a modern speleothem from southwest Australia. Earth and Planetary Science Letters 233, 17–32. https://doi.org/10.1016/j.epsl.2005.02.013

Tudurí, E., Ramis, C., 1997. The Environments of Significant Convective Events in the Western Mediterranean. Wea. Forecasting 12, 294–306. https://doi.org/10.1175/1520-0434(1997)012<0294:TEOSCE>2.0.CO;2

Tyler, J.J., Jones, M., Arrowsmith, C., Allott, T., Leng, M.J., 2016. Spatial patterns in the oxygen isotope composition of daily rainfall in the British Isles. Clim Dyn 47, 1971–1987. https://doi.org/10.1007/s00382-015-2945-y

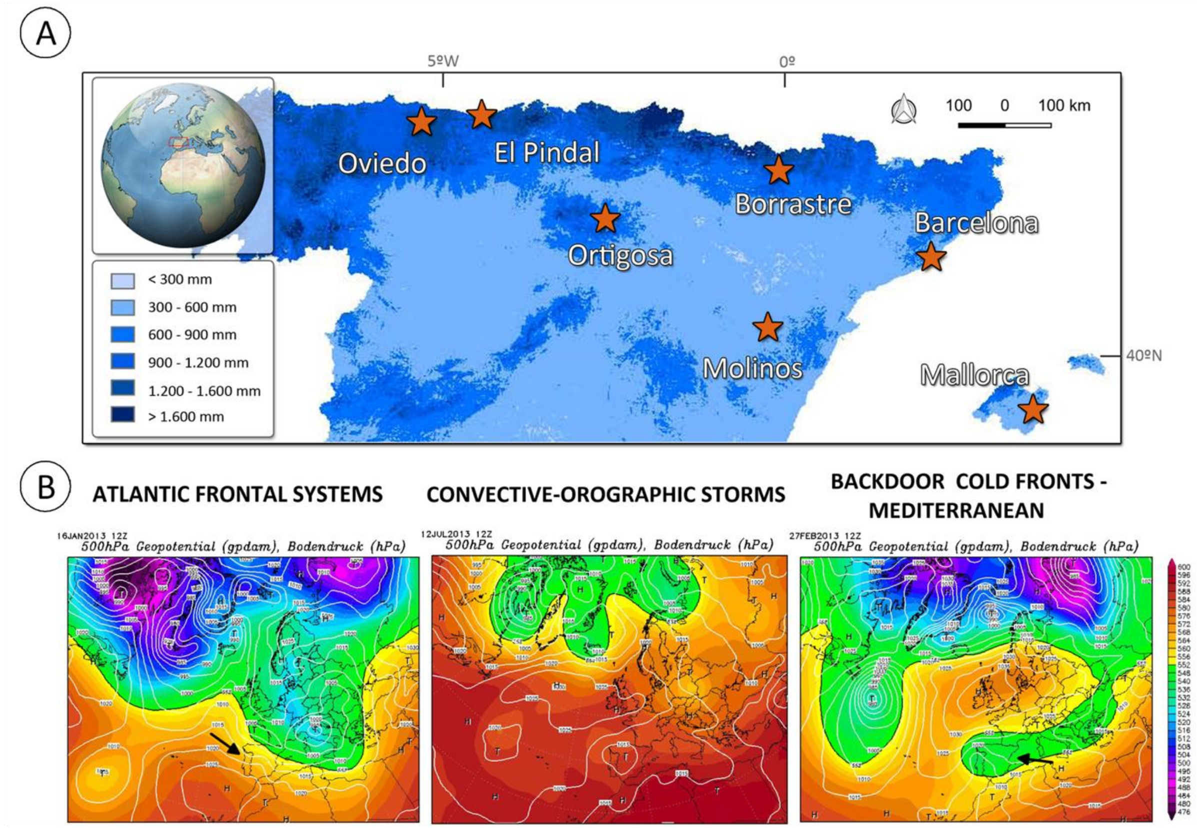

Figure 1. (A) Location of the studied stations in northern Spain where rainfall was collected. Map source: Average annual precipitation (mm) for 1980-2005 provided by the Spanish Ministry of Agriculture and Fisheries, Food and Environment (MAPAMA); (B) weather maps showing the three precipitation regimes of the IP defined by Millán et al. (2005): (i) Atlantic frontal systems, (ii) convective–orographic storms, and (iii) Backdoor cold fronts from the Mediterranean Sea. In the maps, the sea level pressure and the 500 hPa geopotential height (gpdam in German) are indicated by the different colors; the scale represents the height- from 4600 to 6000 m - where the pressure of 500hPa is reached. White lines are the isobars (bodendruck in German). Source: CFS Reanalysis (CFSR) and Wetterzentrale.

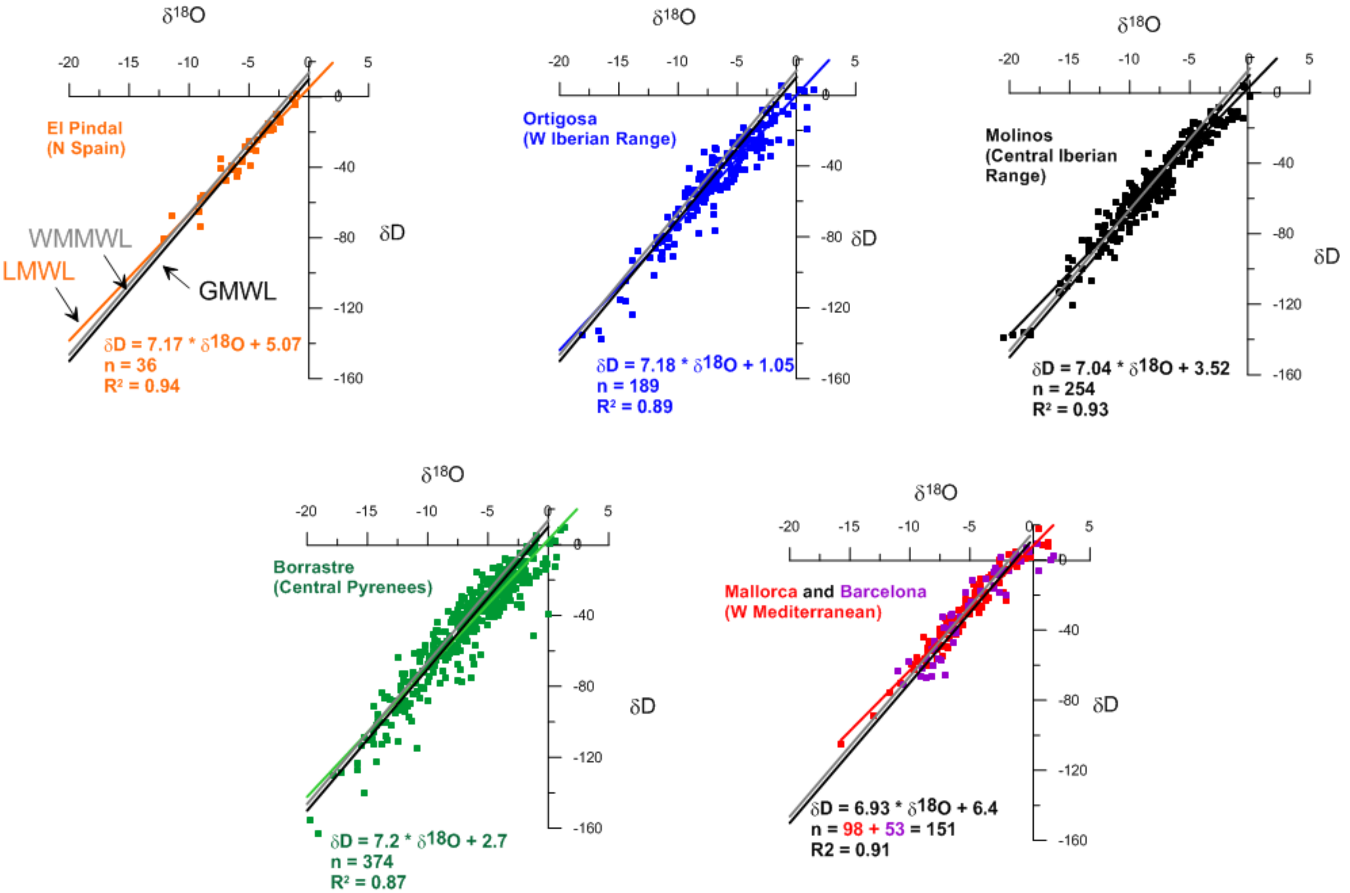

Figure 2. Scatter plots of δ^2H_p versus $\delta^{18}O_p$ in precipitation and Local Meteoric Water Lines (LMWL), including equations, for El Pindal, Ortigosa de Cameros, Borrastre, Molinos and Mallorca with Barcelona stations. Note that El Pindal plot includes only 36 samples since δ^2H was not measured in the remaining samples. The difference in the other graphs in sample number (n) respect to those indicated in Table S1 is due to the removal of some samples that have been subject to evaporation effects (see text for more information). Global Meteoric Water Line (GMWL) and Western Mediterranean Meteoric Water Line (WMMWL) are plotted in black and gray, respectively, in every graph.

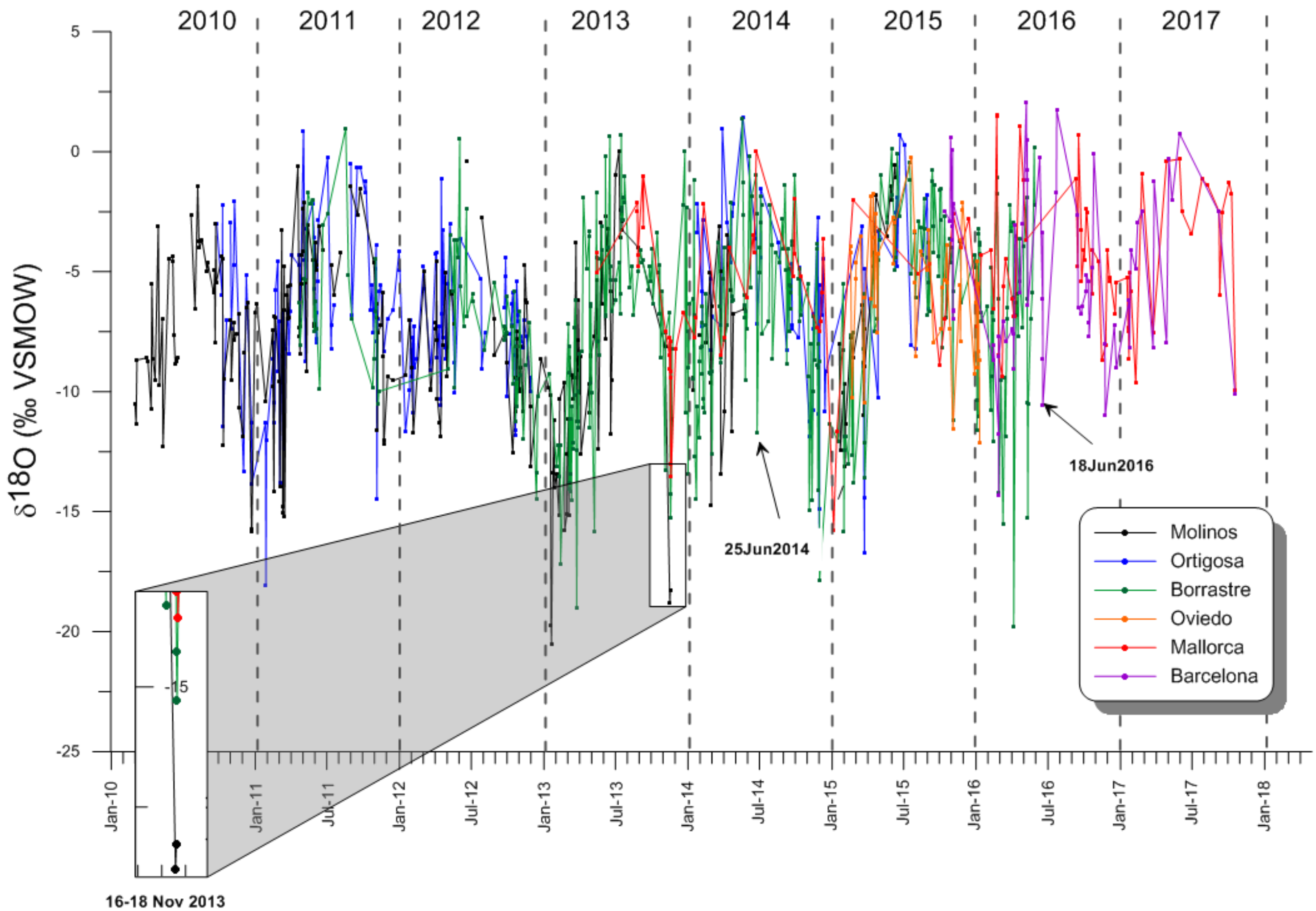

Figure 3. $\delta^{18}O_p$ daily time series for the studied stations presented versus time (2010-2017). Note that El Pindal samples (2006-2009) are not represented since they do not overlap with the time period of the other stations. See text for more explanation.

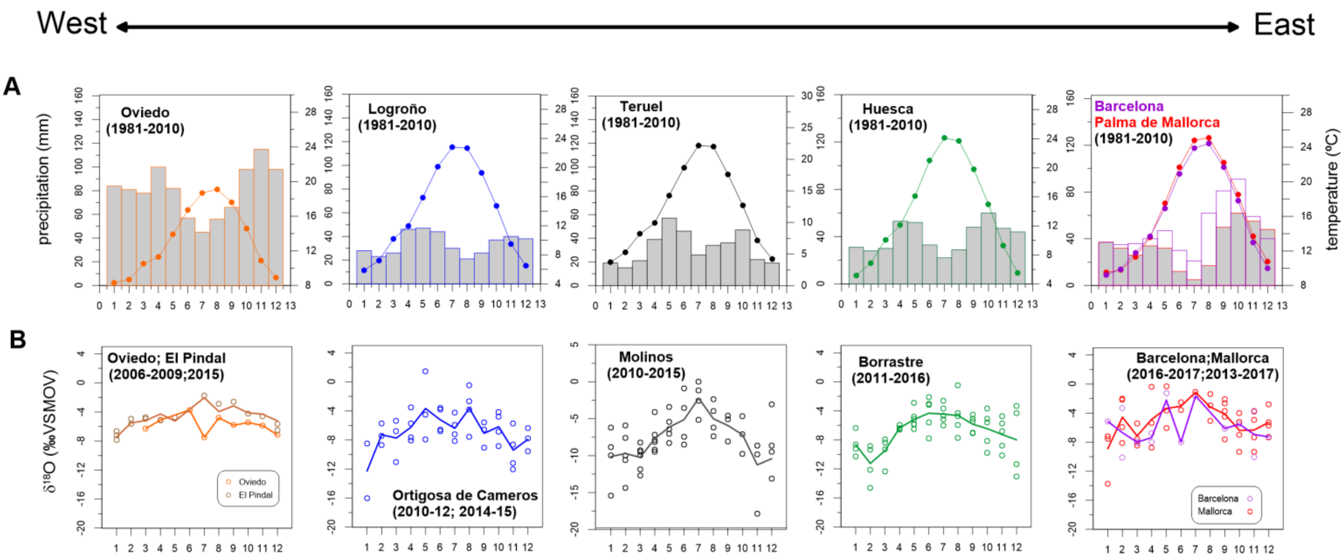

Figure 4. (A) Climographs showing monthly mean temperature (line with dots) and monthly mean rainfall (bars) obtained for the longest AEMET meteorological stations available next to the study sites (Oviedo, Logroño, Teruel, Huesca, Barcelona and Palma de Mallorca). Note that these stations are not at the same elevation or microclimate as the ones where rainfall was collected. For this reason, the climographs are indicated here to account for broad regional climates while the correlations (Table3) with meteorological data were performed using more proximal (although shorter in the recorded time interval) stations. (B) Variability of monthly weighted $\delta^{18}O_p$ at the studied sites. Dots represent monthly precipitation-amount weighted averages and lines are the mean of these monthly precipitation-amount weighted averages (see also Table 2 and Table S2).

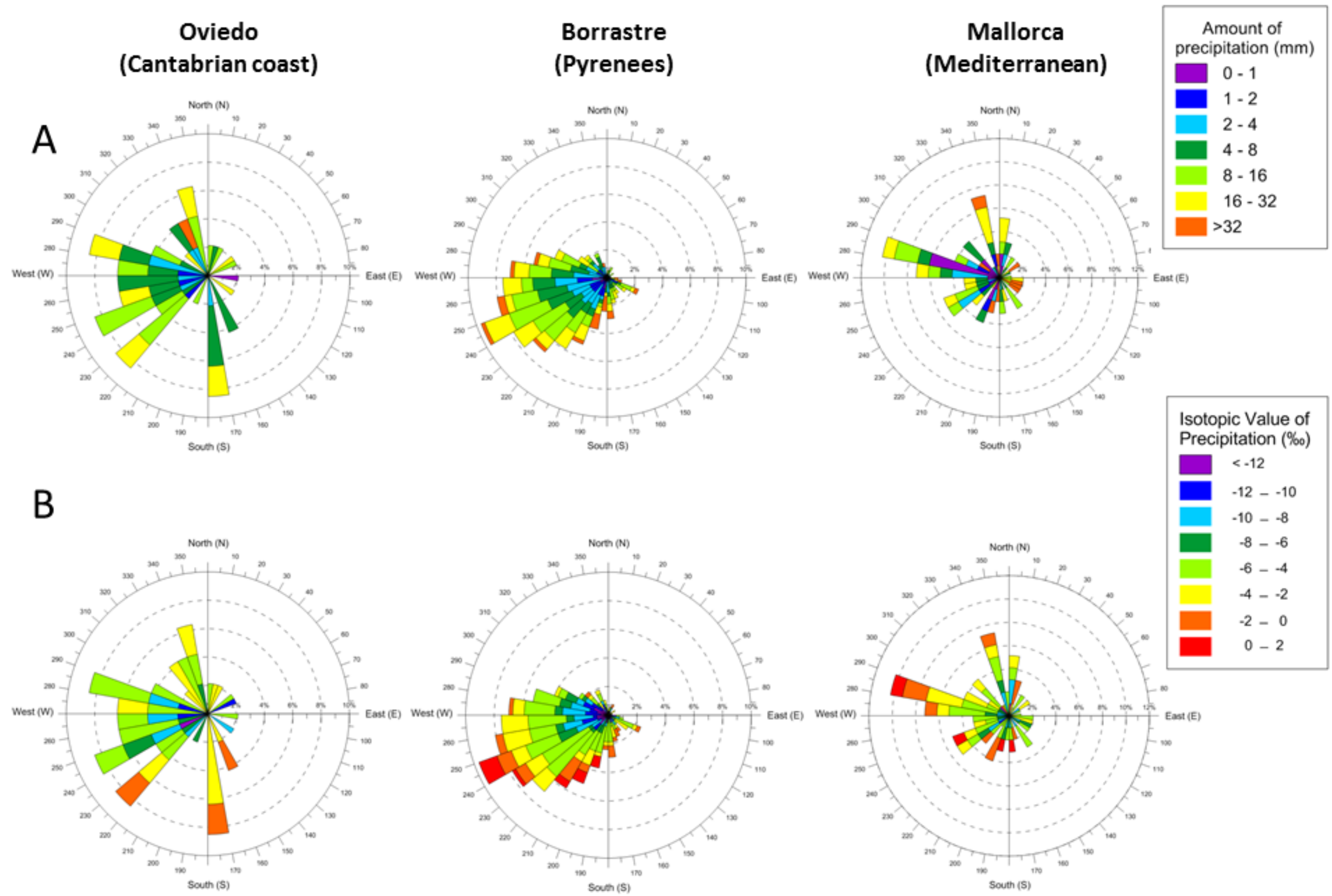

Figure 5. Wind roses showing the averaged back trajectories directions over 24 h life time whose air masses produced precipitation in three stations in northern Iberia: Oviedo (northern Spain), Borrastre (central Pyrenees) and Mallorca (Balearic Islands). (A) Amount of precipitation (measured at the nearest meteorological station) during the intervals of sample collection and (B) $\delta^{18}O_p$ indicated by colors (see legends). Source regions of each air mass, generated by averaging the direction of each point of the back trajectory (20 points), are divided into 10º sectors. The percentages of back trajectories, whose averaged directions are associated with each 10º sector, are shown as dashed circles (from 0 to 12%).

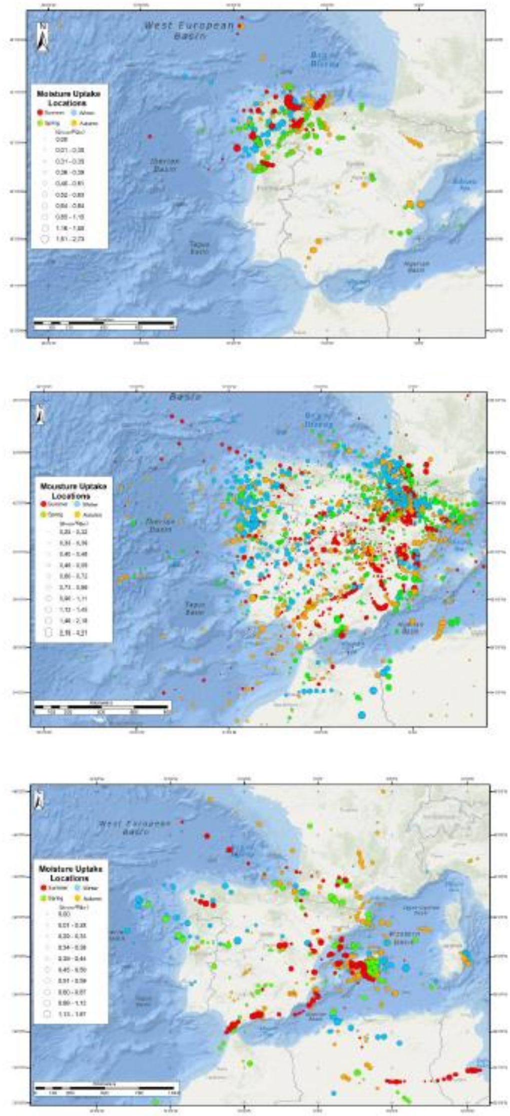

Figure 6. Maps of moisture uptake locations along rainfall backward trajectories represented for Oviedo, Borrastre and Mallorca stations. See legend for colors (indicating seasons) and dot sizes (indicating amount of moisture).

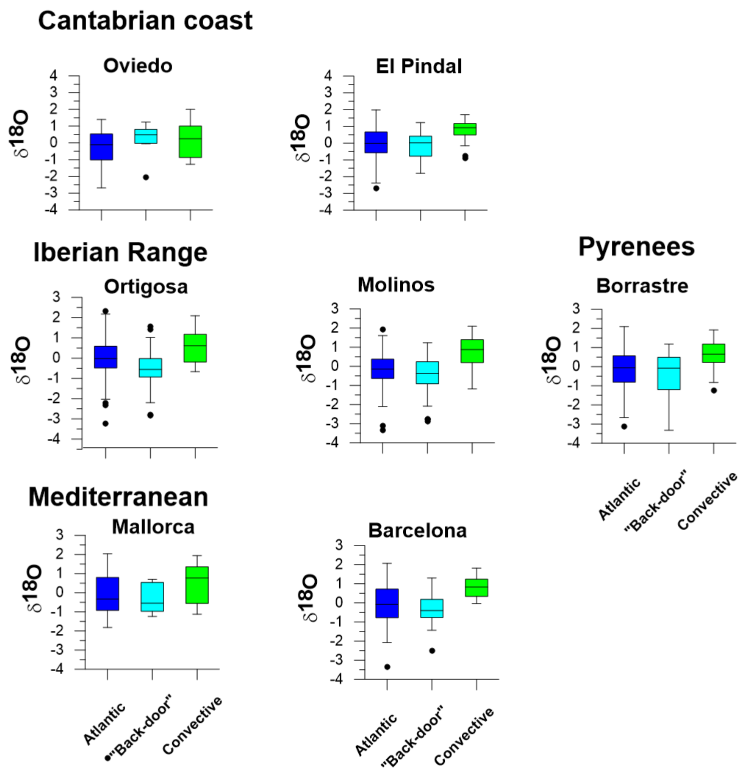

Figure 7. Box plots of $\delta^{18}O_p$ for the three identified rainfall types in northern Iberia: Atlantic fronts (in dark blue), backdoor cold fronts (light blue) and convective precipitation (in green) for the studied stations. The central rectangle spans the first quartile to the third quartile (the *likely range of variation*, the *IQR*). A segment inside the rectangle shows the median and "whiskers" above and below the box show the locations of the minimum and maximum. Values of $\delta^{18}O_p$ appear normalized to better compare among the seven stations. The Kruskal-Wallis test indicates that at least two of the three rainfall types are significantly different in terms of their $\delta^{18}O_p$ values.

Table captions

Table 1. Data collection details for the seven studied stations. KGC: Köppen and Geiger climate classification; AEMET: Agencia Española de Meteorología; SAIH: Automatic Hydrologic Information System. See Table S1 for all the isotopic and meteorological data. The AEMET stations with long series represented in Figure 4A are indicated.

Rainfall collection site									Meteorological data				
Location		***Coordinates and altitude***			***KGC***	***Data description***			***Station***		***Annual mean Temp (°C)***	***Annual rainfall (mm)***	***AEMET long series (with data from 1981-2010)***
		Lat	*Long*	*Altitude m asl*		*Collection period*	*Nº samples*	*Laboratory*	*Name*	*Type*			
Cantabrian coast	*Oviedo*	43°21N	5°51W	245	Cfb	Feb 2015-Jan 2016	47	Universities. of Oviedo and Barcelona (UB)	Oviedo (120 km from El Pindal)	AEMET	13.3	960	Oviedo
	El Pindal	43°23N	4°31W	24	Cfb	Nov 2006-Feb 2007 July 2007-May 2008 Jan 2009-April2009	101		Data from reanalysis (ECWMF ERA interim data)				
Iberian Range	*Ortigosa de Cameros*	42°10N	2°42W	1060	Dsb	Sep 2010–Dec 2014	189	IACT-CSIC and UB	Villoslada de Cameros (6.5 km)	La Rioja govern	9.6	650	Logroño
	Molinos	40°47N	0°26W	1040	Dsb	March 2010-May 2015	254	IACT-CSIC	Gallipuén (7 km)	SAIH Ebro	12	500	Teruel
Pyrenees	*Borrastre*	42°29N	0°06W	770	Csb	Since April 2011	374		Borrastre (in situ)	Meteo-climatic	13.5	900	Huesca
Mediterreanean	*Barcelona*	41°21N	2°06E	20	Csa	Since Oct 2015	53	UB	Barcelona-Zona Universitaria (in situ)	meteocat	17.2	430	Barcelona
	Mallorca (Manacor and Porto Cristo)	39°33N	3°12E	90	Csa	Since May 2013	98		Sant Llorenç (8 km)	AEMET	18.8	590	Palma de Mallorca

Table 2. Mean values of $\delta^{18}O_p$ data for every station in the study transect at a monthly and annual scale. Only months and years with all events collected are averaged. Note that the number of months or years averaged (number between brackets after the $\delta^{18}O_p$ values) are not the same for all the stations, neither the time period considered (check Table 1 for the sampling period in every station). For the complete monthly dataset with all the monthly values indicated, please see Table S2.

$\delta^{18}O_p$ (‰)	*Cantabrian coast*		*Iberian Range*		*Pyrenees*	*Mediterranean*	
	Oviedo	**El Pindal**	**Ortigosa de Cameros**	**Molinos**	**Borrastre**	**Barcelona**	**Mallorca**
January		-7.46 (3)	-12.29 (2)	-10.12 (4)	-8.64 (4)	-5.15 (1)	-8.91 (4)
February		-5.49 (2)	-7.28 (3)	-9.71 (5)	-11.25 (4)	-6.71 (2)	-4.57 (4)
March	-6.29 (1)	-5.19 (2)	-7.74 (3)	-10.25 (6)	-9.49 (4)	-8.00 (2)	-7.15 (3)
April	-5.12 (1)	-4.27 (2)	-6.25 (4)	-7.68 (6)	-6.35 (4)	-7.38 (2)	-4.86 (3)
May		-5.25 (1)	-3.66 (3)	-6.13 (5)	-5.19 (6)	-2.21 (2)	-3.36 (3)
June	-3.73 (1)		-5.21 (4)	-5.12 (4)	-4.32 (5)	-8.01 (1)	-3.06 (2)
July	-7.50 (1)	-2.04 (1)	-6.39 (4)	-2.22 (4)	-4.44 (5)	-1.64 (1)	-1.13 (1)
August	-4.80 (1)	-3.94 (1)	-3.64 (4)	-5.00 (4)	-4.65 (5)		-3.15 (3)
September	-5.83 (1)	-3.17 (1)	-7.09 (3)	-5.93 (3)	-5.83 (5)	-6.13 (1)	-4.14 (5)
October	-5.47 (1)	-4.12 (1)	-6.17 (4)	-7.18 (3)	-6.46 (5)	-5.53 (1)	-6.38 (4)
November	-5.87 (1)	-4.31 (1)	-9.40 (4)	-11.26 (4)	-7.24 (5)	-6.95 (2)	-6.34 (4)
December	-7.16 (1)	-5.23 (2)	-7.91 (3)	-10.41 (3)	-8.00 (4)	-7.27 (1)	-5.28 (4)
Annual			-7.09 (1)	-7.18 (2)	-6.37 (3)		

Table 3. Spearman´s rank correlation coefficients between $\delta^{18}O_p$ and air temperature and precipitation amount for every sampling station at daily scale (A) and monthly scale (B) using deseasonalized data (removing the seasonal component by subtracting their monthly averages). Significant correlations with *p value* < 0.05 after application of *Bonferroni test* are in italics. Note that the relatively small size of Oviedo and Barcelona rain events likely precludes statistically significant correlations. (C) Multiple regression coefficient (r) and *p-value* for every site is included, indicating the coefficient and the standard error for the constant, the precipitation and the air temperature variables. As an example, the equation for Molinos should be read as follows: $\delta^{18}O_p$=– 0.05(±0.019) *A* +0.40(±0.05) *T* + 0.43, with *A* as the amount of precipitation, *T* as air temperature and 0.43 as a constant value.

		Oviedo	El Pindal	Ortigosa de Cameros	Molinos	Borrastre	Barcelona	Mallorca
(A) Daily correlations		n = 39	n = 109	n=189	n=248	n=352	n=53	n=98
$\delta^{18}O_p$ - temperature	r_s	0.23	0.34	0.25	0.41	0.31	0.24	0.35
	p value	0.328	0.0012	0.001	2.00E-11	1.17E-09	0.21	0.0013
$\delta^{18}O_p$ - precipitation amount	r_s	-0.22	-0.06	-0.32	-0.19	-0.11	-0.35	-0.28
	p value	0.368	1	1.05E-05	0.005	0.119	0.029	0.013
(B) Monthly correlations		n = 9	n = 17	n=41	n=51	n=49	n=16	n=40
$\delta^{18}O_p$ - temperature	r_s	0.3	0.33	0.46	0.76	0.61	0.39	0.41
	p value	1	1	0.013	3.36E-10	1.44E-05	0.804	0.05
$\delta^{18}O_p$ - precipitation amount	r_s	0.066	-0.44	-0.34	-0.4	-0.11	-0.30	-0.12
	p value	0.843	0.4	0.176	0.018	1	1	0.436
(C) Multiple regression (with daily data)	r	0.30	0.40	0.40	0.43	0.30	0.32	0.41
	p value	0.118	0.0001	3.36E-08	4.68E-13	8.13E-09	0.004	0.008
Constant	Coeff	0.14	0.32	-1.6	0.43	-2.83E-11	-0.49	0.23
	Std err	0.43	0.24	0.22	0.18	0.16	0.38	0.26
Precipitation	Coeff	-0.015	-0.013	-0.11	-0.05	-0.018	-0.05	-0.02
	Std err	0.05	0.04	0.02	0.019	0.014	0.02	0.017
Temperature	Coeff	0.21	0.25	0.25	0.40	0.40	0.37	0.31
	Std err	0.11	0.05	0.06	0.05	0.06	0.19	0.11

Table 4. Relative frequency (in %) of the three rainfall types in every studied station.

	Cantabrian coast		*Iberian Range*		*Pyrenees*	*Mediterranean*	
	Oviedo	**El Pindal**	**Ortigosa de Cameros**	**Molinos**	**Borrastre**	**Barcelona**	**Mallorca**
Atlantic fronts	68.09	71.29	58.7	51.8	65.2	58.49	40.82
Backdoor cold fronts	14.89	16.83	20.6	23.9	11.8	24.53	38.78
Convective	17.02	11.88	20.6	24.3	23.0	16.98	20.41

Tabla 5. Kruskal-Wallis test performed on $\delta^{18}O_p$ data to discriminate if the three synoptic patterns are statistically different in terms of their isotopic composition. High values of the test (Kruskal-Wallis H) and low *p-valu*es indicate that at least two of the three synoptic patterns are statistically different in terms of $\delta^{18}O_p$ data.

	Cantabrian coast		*Iberian Range*		*Pyrenees*	*Mediterranean*	
	Oviedo	**El Pindal**	**Ortigosa de Cameros**	**Molinos**	**Borrastre**	**Barcelona**	**Mallorca**
Kruskal-Wallis *H*	3.017	10.86	23.3	48.38	47.84	4.109	22.23
p value	0.221	0.004	8.7E-06	3.12E-11	4.09E-11	0.1282	1.49E-05

Supplementary

Figure S1. Wind roses represent the averaged back trajectories of air masses that produced precipitation at three stations in northern Iberia: Oviedo (northern Spain), Borrastre (central Pyrenees) and Mallorca (Balearic Islands). Trajectories shown were computed for 120 hours.

As supplementary

Figure S2. Oviedo station. From top to bottom: daily precipitation (mm), $\delta^{18}O$ (‰) and daily air temperature average (ºC).

Figure S3. El Pindal station. From top to bottom: daily precipitation (mm), *d-excess*, $\delta^{18}O$ (‰) and daily air temperature average (ºC).

Figure S4. Ortigosa station. From top to bottom: daily precipitation (mm), *d-excess*, $\delta^{18}O$ (‰) and daily air temperature average (ºC).

Figure S5. Molinos station. From top to bottom: daily precipitation (mm), *d-excess,* $\delta^{18}O$ (‰) and daily air temperature average (ºC).

Figure S6. Borrastre station. From top to bottom: daily precipitation (mm), *d-excess*, $\delta^{18}O$ (‰) and daily air temperature average (ºC).

Figure S7. Barcelona station. From top to bottom: daily precipitation (mm), *d-excess*, $\delta^{18}O$ (‰) and daily air temperature average (ºC).

Figure S8. Mallorca station. From top to bottom: daily precipitation (mm), *d-excess*, $\delta^{18}O$ (‰) and daily air temperature average (ºC).

Table S1. Event $\delta^{18}O_p$ and δ^2H_p data for the stations considered in this study. Meteorological data from nearby stations (Table 1) are also included.

As supplementary

Table S2. Monthly $\delta^{18}O_p$ data for the stations considered in this study

As supplementary